REVIEW

*National Science Open*
5: 20260015, 2026
https://doi.org/10.1360/nso/20260015

Materials Science

Special Topic: Hollow Multishelled Structure

# Hollow-structured nanoplatforms for photothermal synergistic therapy in bacterial infections

Naixin Kang[1,2], Decai Zhao[1,*], Jiawei Wan[1] & Dan Wang[3,*]

[1]*State Key Laboratory of Biopharmaceutical Preparation and Delivery, Institute of Process Engineering, Chinese Academy of Sciences, Beijing 100190, China;*
[2]*School of Chemical Engineering, University of Chinese Academy of Sciences, Beijing 100049, China;*
[3]*College of Chemistry and Environmental Engineering, Shenzhen University, Shenzhen 518071, China*

*Corresponding authors (emails: dczhao@ipe.ac.cn (Decai Zhao); danwang@szu.edu.cn (Dan Wang))

Received 28 January 2026; Revised 3 April 2026; Accepted 16 April 2026; Published online 17 April 2026

**Abstract:** In recent years, due to the commonality of bacterial infections and the emergence of antimicrobial resistance, non-invasive photothermal therapy (PTT) has been increasingly recognized as an effective antibacterial strategy with distinct advantages. Hollow-structured photothermal nanoplatforms are capable of not only enhancing photothermal performance but also serving as multifunctional antibacterial systems through cavity-enabled drug loading and diverse functional components, thus integrating multiple therapeutic modalities in a single platform and exhibiting substantial potential in antibacterial applications. In this review, the design and synthesis strategies of hollow-structured antibacterial materials are summarized, with a particular focus on their photothermal enhancement mechanisms and structure-property relationships. Additionally, the latest advances in hollow-structured photothermal therapy are discussed from the perspectives of diverse synergistic strategies and application scenarios. Finally, the current challenges and future perspectives are highlighted, where intelligent design and large-scale fabrication are expected to pave the way for antibacterial synergistic therapy of hollow structures.

**Keywords:** hollow-structured, photothermal, antibacterial

## INTRODUCTION

Bacterial infections are common in daily life, ranging from minor abrasions to surgical incisions. Bacterial infections lead to delayed wound healing and even pose life-threatening risks, thereby recognized as a major global public health challenge that urgently requires an effective solution [1,2]. Although antibiotics have been the most effective treatment for bacterial infections for decades, their overuse has led to the emergence of serious challenges such as antimicrobial resistance (AMR) [3]. More critically, bacteria are prone to adhere to biotic or abiotic surfaces and subsequently form structured, three-dimensional communities enveloped by extracellular macromolecules—known as biofilms [4]. Biofilm formation impedes antibiotic penetration and exhibits high levels of drug resistance, phagocytosis evasion, and adhesion capability [5–7]. Furthermore, systemic side effects, such as intestinal dysbiosis and toxicity [8,9], can be readily induced by excessive antibiotic use. Consequently, the development of safe and effective novel antibacterial strategies

for treating bacterial infections is urgently required [10].

In response to challenges such as AMR, a series of non−antibiotic−based antibacterial approaches have been developed, such as bacteriophages [11,12], phototherapy [13–15] and antimicrobial peptides [16,17]. Among these, photothermal therapy (PTT) has emerged as a particularly promising antibacterial modality and has attracted considerable attention. PTT is based on photothermal agents (PTAs), which convert light energy into heat under irradiation at specific wavelengths, resulting in a localized temperature increase capable of damaging bacterial cell membranes, killing bacteria, and disrupting the biofilm matrix [18]. The therapeutic temperature can be precisely regulated by adjusting the irradiation time and power, enabling spatiotemporally controllable treatment at designated sites. Moreover, the bactericidal effect of PTT is based on a physical thermal mechanism, which minimizes the risk of inducing bacterial resistance, indicating non-invasive, safe, and highly efficient therapeutic advantages. Nevertheless, monotherapy based on PTT is subject to inherent limitations. First, the therapeutic efficacy of PTT is highly temperature-dependent: insufficient heating may result in inadequate antibacterial effects, whereas excessive temperatures (>60 °C) can cause damage to surrounding healthy tissues. In practice, real-time and precise monitoring and control of local temperature during treatment remain technically challenging. Second, due to the physical barrier and thermal insulation effect of the extracellular polymeric substance (EPS) matrix in biofilms, single PTT exhibits limited efficacy in biofilm eradication. Third, the application of PTAs in deep−tissue infections is restricted by limited light penetration depth. As a result, photothermal-synergistic therapeutic strategies have become a research focus [19–21]. By integrating PTT with complementary modalities such as photodynamic therapy (PDT), gas therapy and chemodynamic therapy (CDT), the limitations of standalone PTT can be overcome, thereby achieving enhanced and complementary therapeutic effects.

The rapid advancement of nanotechnology has provided new opportunities for the application of nanomaterials in the treatment of bacterial infection [22]. Among them, hollow-structured nanomaterials are recognized as one of the current research hotspots in antibacterial applications. Featuring an internal cavity, hollow structures enable the high-capacity loading of antibacterial agents [23,24], including antibiotics and metal ions. In addition, hollow structures can be rationally engineered to possess photothermal conversion capability or enzyme-mimetic activity, enabling synergistic antibacterial effects between the material itself and the loaded drugs [25,26]. Furthermore, surface functionalization of hollow structures facilitates bacterial targeting and stimuli-responsive drug release [27,28]. Therefore, hollow-structured materials hold great promise as multifunctional antibacterial platforms. Hollow-structured photothermal platforms are also particularly attractive for biofilm-associated infections. The difficulty in treating biofilms primarily stems from the physical barrier of the EPS matrix, the negatively charged surface of biofilms, and the complex microenvironment. These factors collectively limit the penetration, accumulation, and efficacy of drugs, reactive oxygen species (ROS), etc. Hollow-structured photothermal platforms offer unique advantages in addressing these challenges in biofilm infections. On the one hand, the photothermal effect can loosen the EPS, reduce biofilm adhesion, and increase bacterial membrane permeability. On the other hand, strategies enabled by the hollow structure, such as charge reversal, cationic modification, enzyme-responsive gating, and pH-responsive release, enable targeted bacterial membrane interaction, enhanced local adhesion, and deep delivery capabilities. Therefore, the therapeutic value of hollow-structured photothermal platforms lies not only in photothermal ablation itself but also in their comprehensive ability to overcome biofilm-associated barriers.

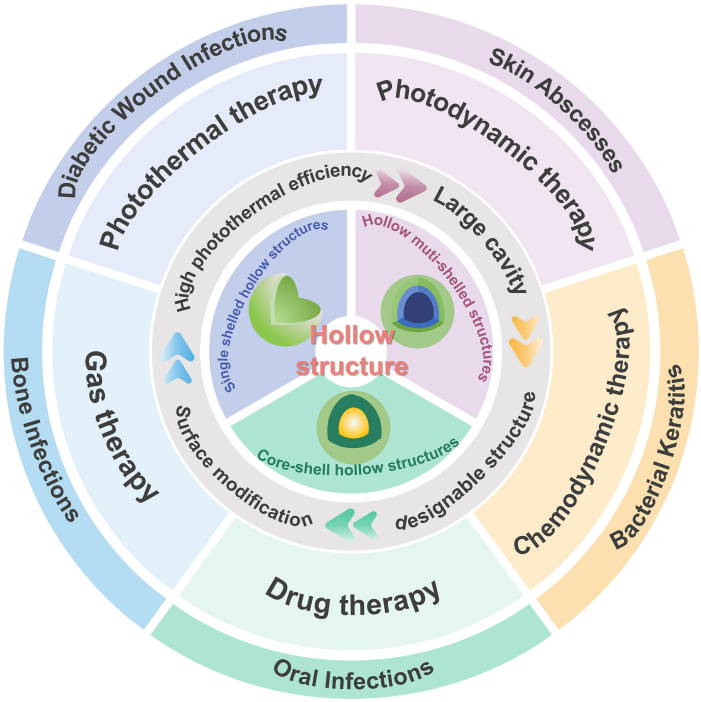


**Figure 1** Schematic illustration of photothermal synergistic therapy strategies based on hollow structures for multiple infection scenarios. Four layers of construction in hollow structure are shown from the core outward: classification of hollow architectures, key advantages of hollow structures as photothermal antibacterial platforms, combinatorial strategies integrating photothermal therapy with other therapeutic modalities, and applications of hollow-structured photothermal antibacterial platforms across diverse treatment scenarios.

In this review, we systematically summarize recent advances in hollow-structured photothermal antibacterial nanoplatforms by integrating materials design strategies, synergistic antibacterial strategies and applications in disease therapy. We first outline the design and synthesis strategies of hollow-structured photothermal antibacterial materials, highlighting hollow-architecture-enabled photothermal enhancement mechanisms, structure-property relationships, and versatile synthesis routes. Next, diverse photothermal-synergistic antibacterial strategies enabled by hollow nanoplatforms are discussed, including combinations with PDT, CDT, drug therapy, and gas therapy, together with their applications and mechanisms of enhanced efficacy in combination with PTT. Furthermore, advances in the application of hollow-structured nanoplatforms, ranging from superficial wound infections to deep-seated infections, are reviewed, demonstrating the feasibility and considerable potential of photothermal-synergistic treatment for complex infectious scenarios. Finally, the remaining challenges related to scalable fabrication, clinical translation, and biosafety concerns are addressed, and further perspectives are proposed (Figure 1).

## DESIGN AND SYNTHESIS STRATEGIES OF HOLLOW-STRUCUTRED PHOTOTHERMAL ANTIBACTERIAL MATERIALS

Hollow structures, characterized by their large internal cavities, high specific surface area, and tunable shells, exhibit tremendous potential in the field of photothermal antibacterial therapy. To achieve specific func-

tionalities such as efficient photothermal conversion and sequential drug release, the design of component selection, structural architecture, and surface functionalization is paramount. This chapter mainly illustrates design and synthesis strategies of hollow-structured photothermal antibacterial materials. The chapter first outlines the fundamental principles of photothermal antibacterial therapy. Then, the photothermal performance enhancement mechanisms of hollow structures are critically analyzed from four aspects, i.e., enhanced light harvesting, enhanced localized surface plasmon resonance effect, reduced charge recombination, and large specific surface area, underscoring the distinctive advantages of hollow structures as photothermal nanoplatforms. The structural classification, functional customization strategies, and synthesis approaches of hollow-structured photothermal antibacterial materials are subsequently categorized, establishing the material and theoretical basis for the rational design of multifunctional photothermal synergistic antibacterial platforms.

## Photothermal antibacterial mechanisms

When exposed to temperatures above approximately 45 °C, the viability of most bacteria is significantly compromised. As illustrated in Figure 2a [29], depending on the type of PTAs, different photothermal conversion mechanisms are involved, including localized surface plasmon resonance (LSPR) in metals, photoinduced electron-hole generation and relaxation processes in semiconductors, as well as the highest occupied molecular orbital (HOMO)-lowest unoccupied molecular orbital (LUMO) excitation and lattice vibrations in molecular systems [30,31]. Through these mechanisms, PTAs efficiently absorb incident light at specific wavelengths and convert it into thermal energy. Part of this heat can be transferred to nearby bacteria, leading to the denaturation of bacterial proteins, disruption of the biomembrane, and ultimately inducing bacterial death. By modulating the composition, structure, morphology, and size of PTAs, together with the wavelength and intensity of incident light, the photothermal antibacterial efficiency can be precisely regulated.

## Mechanisms for enhanced photothermal performance in hollow structures

Compared with solid structure materials, hollow structures exhibit enhanced photothermal conversion performance. It achieves efficient conversion of light energy to heat energy through the synergistic effects of multiple physicochemical mechanisms, including enhanced light-harvesting capability, localized surface plasmon resonance effect and non-radiative relaxation. Furthermore, the high specific surface area associated with hollow structures can also indirectly promote energy dissipation and local heat accumulation by enhancing light scattering and defect state density. However, their effects are more manifested as a synergistic amplification of mechanisms above rather than an independent path for photothermal enhancement.

### *Enhanced light-harvesting capability*

The first step in photothermal conversion is the capture of light. Common strategies to promote light harvesting involve broadening the light absorption range, minimizing light loss upon light transmission, and increasing the optical path length within the material [32]. Hollow structures, particularly hollow multi-

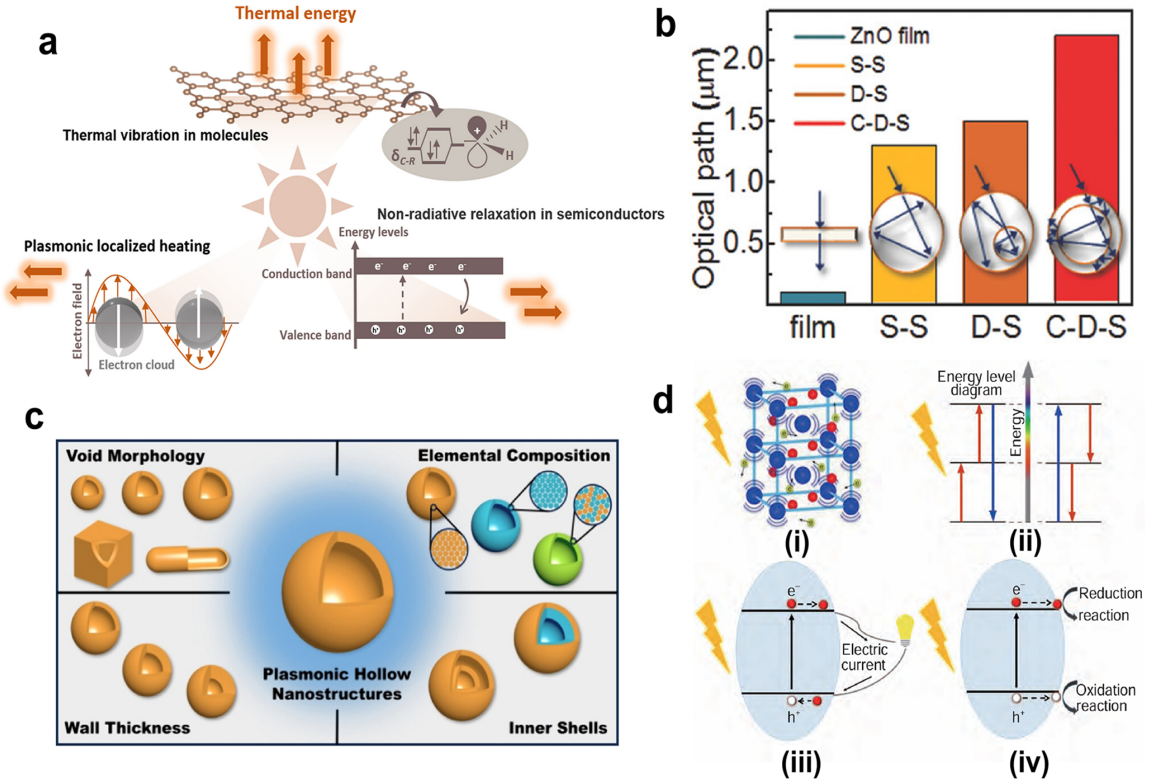


**Figure 2** (a) Different mechanisms of photothermal effect. Reproduced with permission from Ref. [29]. Copyright©2021, Elsevier Inc. (b) The optical path within different types of ZnO PDs and corresponding schematic drawings for the multiple reflection of light within ZnO nanoshell- and film-based devices. Reproduced with permission from Ref. [35]. Copyright©2018, WILEY-VCH. (c) Engineering the internal structure of hollow nanostructures for enhanced plasmonic properties. Reproduced with permission from Ref. [41]. Copyright©2024, American Chemical Society. (d) Several mechanisms of hollow multishelled structures reacted with photons: (i) Photons induce collective excitation of phonons and/or electrons, generating heat energy; (ii) photons are upconverted or down-converted to higher or lower energy, exhibiting photoluminescence; (iii) photons generate photo-induced carriers, and electrons travel through an external circuit, forming an electric current and producing electrical energy; (iv) photons excite electrons and holes, which participate in redox reactions, storing chemical energy. Reproduced with permission from Ref. [43]. Copyright©2019, Science China Press.

shelled structures (HoMS), have been demonstrated to improve light harvesting predominantly through enhanced light scattering [33]. As light passes through the outer thin shell, multiple scattering events are induced within the internal cavity or between multiple shells, thereby prolonging the optical path within the materials and enhancing light harvesting capability. The extent of light scattering can be further regulated by tailoring structural parameters of hollow multishelled structures, such as the number of shells and the inter-shell spacing. For instance, Dong *et al*. [34] utilized carbonaceous microspheres as sacrificial templates to prepare hollow ZnO microspheres with tunable shell numbers and inter-shell distances through a simple programmable heating process. Ultraviolet-visible (UV-vis) diffuse reflectance spectroscopy demonstrated that an increased number of shells resulted in enhanced light scattering, and that structures with closely spaced double shells exhibited stronger light scattering than those with larger shell spacing. Furthermore, Lien *et al*. [35] synthesized ZnO HoMS and investigated the influence of different structures on the light scattering ability. As shown in Figure 2b, the optical path within ZnO HoMS was longer than that of ZnO films. This indicates that HoMS can significantly enhance the material's light capture ability through the scattering effect of light, providing more opportunities for achieving effective light conversion.

### *Enhanced localized surface plasmon resonance effects*

Under light irradiation, photothermal nanoparticles composed of noble metals such as gold and platinum, as well as certain transition metals, are capable of absorbing incident light and generating heat through localized LSPR [36,37]. In this process, the electric field of the incident light interacts with the nanoparticles, exciting the movement of charge carriers within the nanostructure. This energy is subsequently converted into thermal energy, resulting in heat release [38–40].

In some of the metal-based hollow structures, the inner and outer metal surfaces can form a nanoscale plasmonic cavity resonator. The optical resonance established within this nanocavity enables light to be trapped in the active region, thereby enhancing light absorption and effectively improving photothermal conversion performance [35]. In addition to the external surface, hollow nanostructures possess internal surfaces, and modulation of the inner surface plays a critical role in enhancing plasmonic effects. Shao *et al*. [41] systematically investigated the influence of key internal structural parameters of hollow nanostructures on their plasmonic performance (Figure 2c). The results demonstrate that precise control over the morphology of the internal cavity, the elemental composition of the shell, the shell thickness, and the inner-shell architecture enables hollow structures to exhibit higher extinction intensities and a broader tunable range of plasmonic resonance peaks, thereby contributing to enhanced photothermal performance. Moreover, multiple light-scattering events within the hollow structures further amplify the LSPR effect, leading to enhanced photothermal conversion capability.

For hollow structures formed from wide-bandgap semiconductor materials, the incorporation of metal particles, such as gold, silver, or platinum, can be utilized to extend the light absorption range into the visible region through the LSPR effect [42], thereby promoting light absorption.

### *Enhanced non-radiative relaxation*

When light irradiates materials, various physical effects can be induced as a result of the electromagnetic oscillations of the incident wave or inelastic photon, such as the photoelectric effect and the photothermal effect (Figure 2d) [43]. In photothermal conversion, photoexcited electrons do not re-emit energy as light; instead, they transfer energy to lattice vibrations through electron-phonon coupling, thereby generating heat. Hollow structures possess a higher defect density and unique inner and outer surfaces, which facilitate the rapid localization of absorbed optical energy within a confined volume. This enhances electron-phonon coupling and promotes non-radiative relaxation processes, thereby efficiently converting light energy into heat while minimizing energy loss through radiative recombination. Furthermore, constructing heterojunctions within hollow structures can intensify energy dissipation and phonon scattering at the interfaces. This directs energy more effectively into lattice vibrations rather than toward generating separated charges or fluorescence, consequently improving photothermal conversion efficiency [44].

## Design of hollow-structured photothermal antibacterial materials

### *Classification of hollow structures*

Based on the number of cores and shells, hollow-structured photothermal antibacterial materials can be

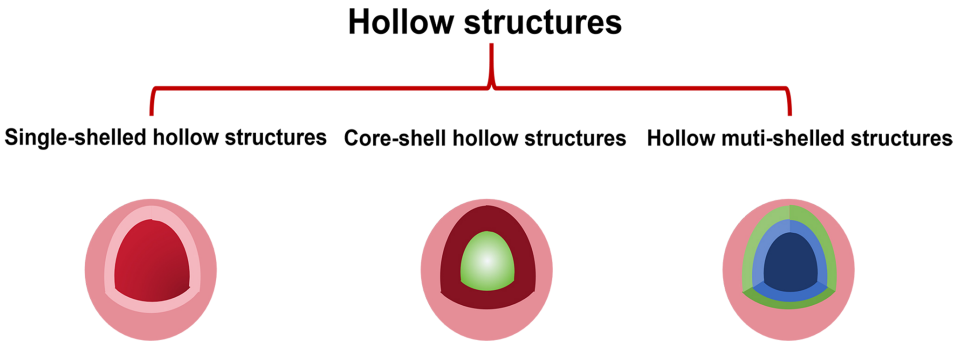


**Figure 3** Classification of hollow structures, including single-shelled hollow structures, core-shell hollow structures and HoMS.

classified into three main categories: single-shelled hollow structures, core-shell hollow structures, and HoMS (Figure 3).

(1) Single-shelled hollow structures. Single-shelled hollow structures are characterized by a single, continuous internal cavity enclosed by an intact shell. Owing to their structural simplicity, high drug-loading capacity, facile surface functionalization, and well-established synthetic routes, single-shelled hollow structures have been extensively explored in biomedical applications. Single-shelled hollow structures are often further engineered or doped to achieve enhanced photothermal antibacterial performance. For instance, He *et al*. [45] developed a manganese-ion-doped Prussian blue hollow structure for photothermal antibacterial applications. By modulating the component ratios of the material, a synergistic balance between optimized photothermal antibacterial activity and controlled thermal damage was achieved, enabling effective bacterial elimination. In addition to exploiting the intrinsic photothermal properties of the material itself, hollow structures can further enhance photothermal performance by utilizing their internal cavities to load large amounts of small-molecule PTAs. For instance, Wu *et al*. [25] fabricated a hollow virus-spike-like $MnO_x$ nanozyme loaded with indocyanine green (ICG). The surface spike structure enhanced bacterial capture capability, while the photothermal effect conferred by ICG disrupted the bacterial biofilms, thereby realizing photothermal-enhanced catalytic therapy for bacterial infection.

(2) Core-shell hollow structures. In contrast to single-shelled hollow structures, core-shell hollow structures refer to a class of hollow structures in which a shell encloses an internal cavity, while a void space is present between the core and the shell. Yolk-shell structures are a specific type of core-shell hollow structure, resembling a “yolk” (core) surrounded by an “eggshell” (shell), without direct contact between the core and the shell. This unique configuration enables the photothermal “yolk” to act as a localized heat center, promoting heat accumulation and reducing thermal dissipation during irradiation. Meanwhile, the surrounding shell and internal void jointly enhance light scattering and thermal confinement, thereby improving photothermal conversion efficiency and sustaining elevated local temperatures at the target site.

Core-shell hollow structures have demonstrated excellent performance in antibacterial applications. For example, Yu *et al*. [46] employed corrole photosensitizers and chitosan as building units and induced the self-assembly of corrole molecules into core-shell photothermal nanoparticles via chitosan templating, driven by hydrogen bonding and π-π stacking interactions, for the treatment of bacterial infections. The corrole photosensitizer was highly aggregated within the core-shell structure, effectively suppressing fluorescence emission and conferring enhanced photothermal properties. Meanwhile, protonated chitosan exhibited a high

positive surface charge, enabling the capture of negatively charged bacteria through electrostatic interactions and exerting its intrinsic antibacterial activity. As a result, synergistic antibacterial therapy combining photothermal effects and inherent antibacterial activity was achieved. In another study, Xiong *et al*. [47] synthesized α-$Fe_2O_3$@Au/Polydopamine (PDA) core-shell nanoparticles via a one-step *in situ* oxidation-redox polymerization method. By varying the concentrations of $HAuCl_4$ and the dopamine precursor, the thickness and composition of the Au/PDA composite shell can be precisely controlled. The α-$Fe_2O_3$@Au/PDA core-shell nanoparticles exhibit superior photothermal bactericidal efficacy against both *Escherichia coli* (*E. coli*) and *Staphylococcus aureus* (*S. aureus*) at low concentrations.

(3) Hollow multishelled structure (HoMS). HoMS are characterized by two or more concentric shells, and their functionality can be finely tuned by adjusting parameters such as the number of shells and the inter-shell spacing. HoMS contains multiple hollow cavities, offering significantly larger specific surface area, pore volume [48] and higher drug loading capacity [49]. Furthermore, the hierarchical light scattering facilitated by the multiple shells enhances light-harvesting capability [50]. HoMS exhibits improved photothermal conversion efficiency and has potential for PTT. For example, Shi *et al*. [51] successfully synthesized triple-shelled hollow mesoporous organosilica nanospheres loaded with copper sulfide. The resulting nanospheres demonstrated high photothermal conversion efficiency and excellent photothermal stability, showing promising prospects for PTT.

### *Functional customization strategies*

Hollow structures for enhancing photothermal performance. Building on the photothermal enhancement mechanisms discussed above, this section focuses on how structural parameters of hollow architectures can be rationally engineered to further optimize photothermal conversion efficiency. During the fabrication of hollow structures via template-assisted or self-templating strategies, key structural parameters including shell number, cavity size, and shell thickness can be precisely regulated by adjusting precursor concentration, template removal rate, and reaction time. An increased number of shells generally leads to a larger specific surface area and higher drug-loading capacity, while the associated multilevel light-scattering effects further enhance light-harvesting capability, thereby improving photothermal conversion efficiency [48]. Figure 4a [52] showed the light scattering for single-shell and double-shell structures, indicating that an increase in the number of shell layers can enhance the light scattering and further improve the light capture capacity.

Compared to solid structures under identical conditions, hollow structures exhibit superior photothermal performance. Liu *et al*. [53] systematically investigated and compared the optical properties and photothermal conversion efficiencies of four plasmonic materials (Ag, Au, Cu, and TiN) in both hollow and solid architectures. The results demonstrated that hollow gold nanorods achieved significantly higher photothermal conversion efficiency, indicating that the hollow structure enhances photothermal performance by promoting both localized and propagating surface plasmon resonances.

(2) Component selection for enhancing photothermal conversion efficiency. Hollow-structured materials with photothermal properties can be classified by their material properties into metal−based materials, semiconductors, carbon-based materials, and organic polymers, each exhibiting unique physicochemical characteristics and photothermal conversion capabilities. Metal-base materials refer to a class of PTAs that rely on the plasmonic resonance effect, primarily including metals and their oxides or sulfides, such as Au

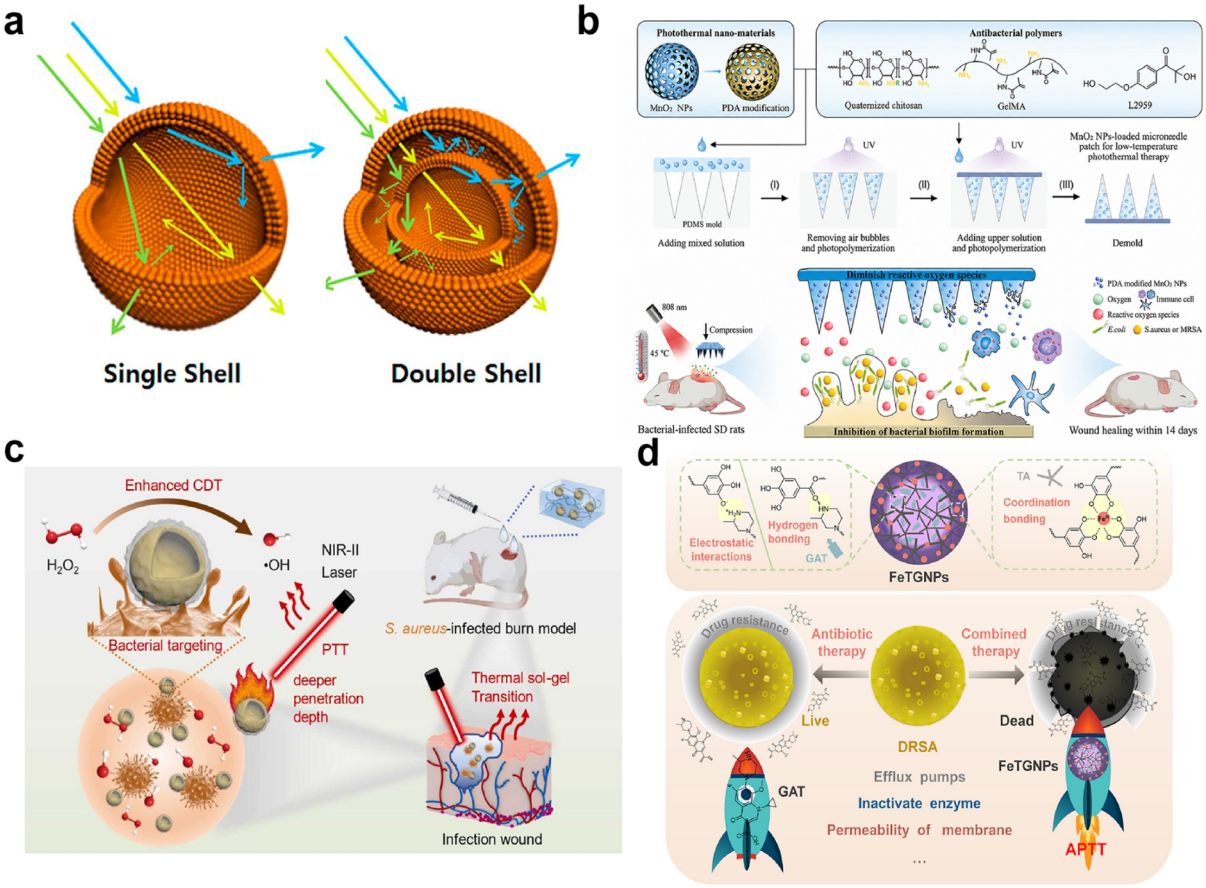


**Figure 4** (a) Schematic diagram of light scattering for single-shell and double-shell hollow structures. Reproduced with permission from Ref. [52]. Copyright©2014, American Chemical Society. (b) Schematic diagram of the preparation and application of PDA-modified $MnO_2$ NPs microneedle patch. Reproduced with permission from Ref. [68]. Copyright©2024, Wiley‐VCH. (c) The application of the thermo-sensitive hydrogel-based composite dressing PHF in the *S. aureus*-infected burn wound model for enhanced NIR-II PTT-CDT synergistic anti-infective therapy. Reproduced with permission from Ref. [73]. Copyright©2023, Elsevier B.V. (d) The chemical structure of the FeTGNPs and the antibacterial application of FeTGNPs. Reproduced with permission from Ref. [74]. Copyright©2021, Elsevier B.V.

[18] and Ag [54]. Photothermal conversion in semiconductors is mainly governed by the plasmonic resonance effect, as observed in metals and their sulfides, such as CuS [55], $MoS_2$ [56]. In carbon-base materials, photothermal conversion arises from the excitation of loosely bound π-electrons followed by their relaxation to the ground state. Representative examples include carbon quantum dots [57,58], graphene [59,60], and carbon nanotubes [61,62]. Similar to carbonsesrials, photot, the absorption of organic polymers in the visible and near−infrared regions originates from the non−radiative relaxation of their abundant delocalized π−electrons, including polydopamine [63] and indocyanine green [64].

For hollow−structured photothermal systems, components from the same or different categories can be selected and combined to achieve specific functionalities. For instance, doping heteroatoms into semiconductors or constructing heterojunctions can modulate the band structure and optimize photothermal conversion efficiency. Yu *et al*. [65] prepared hollow CuS nanoparticles composed of carbon−dot composites, where the hybridization of CuS with carbon dots enhanced the photothermal conversion efficiency. Chen *et al*. [50] synthesized a hollow multishelled structure consisting of carbon and amorphous $Ta_2O_5$. The

incorporation of carbon atoms provided abundant impurity energy levels, enabling broad light absorption. Deng *et al*. [66] designed a hollow CuS@$Cu_2S$@Au satellite nanoparticle. This metal-semiconductor hybrid hetero−nanostructure not only exhibited properties from its individual components but also demonstrated new synergistic photothermal enhancement arising from the interaction between noble-metal plasmonic effects and the semiconductor.

Moreover, introducing functional units with nanozyme activity into the cavity or on the surface of hollow-structured photothermal materials can enhance photothermal antibacterial performance through a synergistic effect. For example, the introduction of enzyme-mimetic components, such as CuO or $MnO_2$, into hollow structures enables CDT functionality [67]. For instance, Chen *et al*. [68] prepared a hollow structure of PDA-coated $MnO_2$ via *in situ* oxidative polymerization and loaded it into the tip layer of microneedles, fabricating a composite double-layer hydrogel microneedle, as shown in Figure 4b. This hydrogel microneedle exhibits remarkable photothermal performance and the introduced $MnO_2$ activates the enzymatic activities of superoxide dismutase (SOD) and catalase (CAT), forming an efficient cascade enzymatic reaction system. This system effectively eliminates ROS generated during PTT, thereby protecting healing tissues from oxidative damage while enabling photothermal antibacterial effects, ultimately promoting wound healing. Moreover, Zhang *et al*. [69] synthesized hollow semimetallic $PtTe_2$ nanorods that exhibited photothermal-responsive antibacterial activity in combination with enzyme-like catalytic behavior, catalyzing endogenous hydrogen peroxide ($H_2O_2$) into oxygen ($O_2$) and hydroxyl radicals (•OH). Through CDT, the photothermal antibacterial effect was further amplified. In another study, Xu *et al*. [70] prepared copper-ion-doped hollow mesoporous polydopamine. Upon copper incorporation, both the photothermal performance and glutathione depletion capability of the hollow mesoporous polydopamine were significantly enhanced, while Fenton-like catalytic activity was simultaneously introduced.

(3) Surface modification for targeted recognition. Targeted recognition can be achieved through surface modification of hollow structures. For example, modifying the surface with agents such as folic acid, antibodies, or peptides enables hollow structures to recognize and target bacteria. For instance, Kong *et al*. [71] prepared $BiO_{1-x}I$ core-shell nanoparticles coated with glycol chitosan and polydopamine, which targeted bacteria at the acidic microenvironment of infected wounds, performing PTT effects. Ye *et al*. [72] developed a hollow mesoporous nanoprobe loaded with indocyanine green to impart photothermal conversion capability. Surface conjugation with $H_2N$-c(RGDfK)-OH (RGD) ensured precise targeting, rendering the nanoprobe suitable for near-infrared II fluorescence image-guided surgery and photothermal therapy. In another study, Wang *et al*. [73] synthesized hollow copper-molybdenum sulfide nanostructures and endowed them with bacterial-targeting ability through modification with a polyethyleneimine-vancomycin conjugate ($P^V$@HCMS) via amide bonding. This functionalization significantly enhanced the synergistic therapeutic efficacy of PTT and CDT. As shown in Figure 4c, a composite dressing composed of the $P^V$@HCMS and a thermosensitive hydrogel poloxamer F127 was further prepared to promote the healing of burn wounds infected with *S. aureus*. The results of the *in vivo* experiments show that this composite hydrogel can effectively inhibit bacteria, promote epithelial regeneration, anti-inflammatory response, collagen deposition and accelerate the healing of burn wounds.

Cavity loading for synergistic antibacterial therapy. The internal cavity of hollow structures can be loaded with various substances, such as antibiotics, photosensitizers, gas precursors, or immune adjuvants, to achieve synergistic treatment effects. Zhang *et al*. [74] synthesized nanoparticles with a core-shell structure

(Figure 4d). The inner core consisted of antibiotics bound with tannic acid, while the outer shell was a photothermal nanoparticle formed by iron ions complexed with tannic acid. The excellent photothermal properties of the outer shell were utilized for photothermal antibacterial effects, and the sustained release of antibiotics from the core enhanced the killing effect on bacteria, achieving synergistic antibacterial effects through PTT and drug therapy. In another example, Xing *et al*. [75] synthesized hollow mesoporous Prussian blue nanoparticles loaded with a photosensitizer (chlorin ester) and integrated them with a hydrogel matrix. This system enabled synergistic antibacterial therapy by combining PTT and PDT.

## Synthesis strategies of hollow-structured photothermal antibacterial materials

### *Hard-template method*

The hard-template method is one of the most commonly used approaches for preparing hollow structures. In this strategy, precursors are deposited onto preformed templates, which are subsequently removed through physical or chemical treatments to yield hollow products. The structure and morphology of the product can be controlled by selecting appropriate templates and regulating the template removal process. The synthesis of hollow structures through hard-template method primarily involves four step [76]: (i) preparation of the desired hard template, (ii) surface modification of the hard template to introduce specific functional groups, (iii) deposition of precursors onto the hard template, and (iv) removal of the hard template through chemical etching, calcination, or other methods to obtain the hollow structures. Commonly used templates in the hard-template method include silica, metal particles, inorganic salts, and biomass, and the technique is relatively mature. Zhang *et al*. [77] synthesized highly crystalline $TiO_2$ hollow spheres composed of nanocrystals via the hard-template method. Carbon spheres were selected as templates, which were removed by calcination in air. Combined with an appropriate deposition method, high-quality $TiO_2$ hollow spheres with polycrystalline shells and excellent robustness were successfully prepared. Based on the hard-template method, Hwang *et al*. [78] fabricated $TiO_2$ HoMS, in which multilayered $SiO_2$ domains served as sacrificial rigid templates and were selectively removed by alkaline etching after $TiO_2$ crystallization, as illustrated in Figure 5a.

In 2009, Wang's group [79] proposed a method for preparing HoMS, known as the sequential templating approach (STA). This method involves a template that plays the role of multiple and sequential templating during its removal. Precursors attached to the template gradually aggregate, solidify, and crystallize, thereby progressively forming multiple robust shells (Figure 5b) [80]. Wei *et al*. [81] directly dissolved titanium tetrachloride and cerium nitrate hexahydrate in acetone to generate titanium and cerium precursors with different particle sizes, which were subsequently converted into HoMS featuring an inner $CeO_2$ shell and an outer $TiO_2$ shell via the sequential templating method. Using a modified STA, Zhang *et al*. [82] reported the first synthesis of multishelled iron single-atom-doped molybdenum disulfide hydride materials through precise compositional control and chemical etching.

### *Soft-template method*

The soft-template method primarily utilizes templates that maintain their specific structure through weak intermolecular or intramolecular interactions, such as micelles, vesicles, and organic macromolecular polymers, which are also easily removed [83]. When the concentration of the templating agent exceeds a

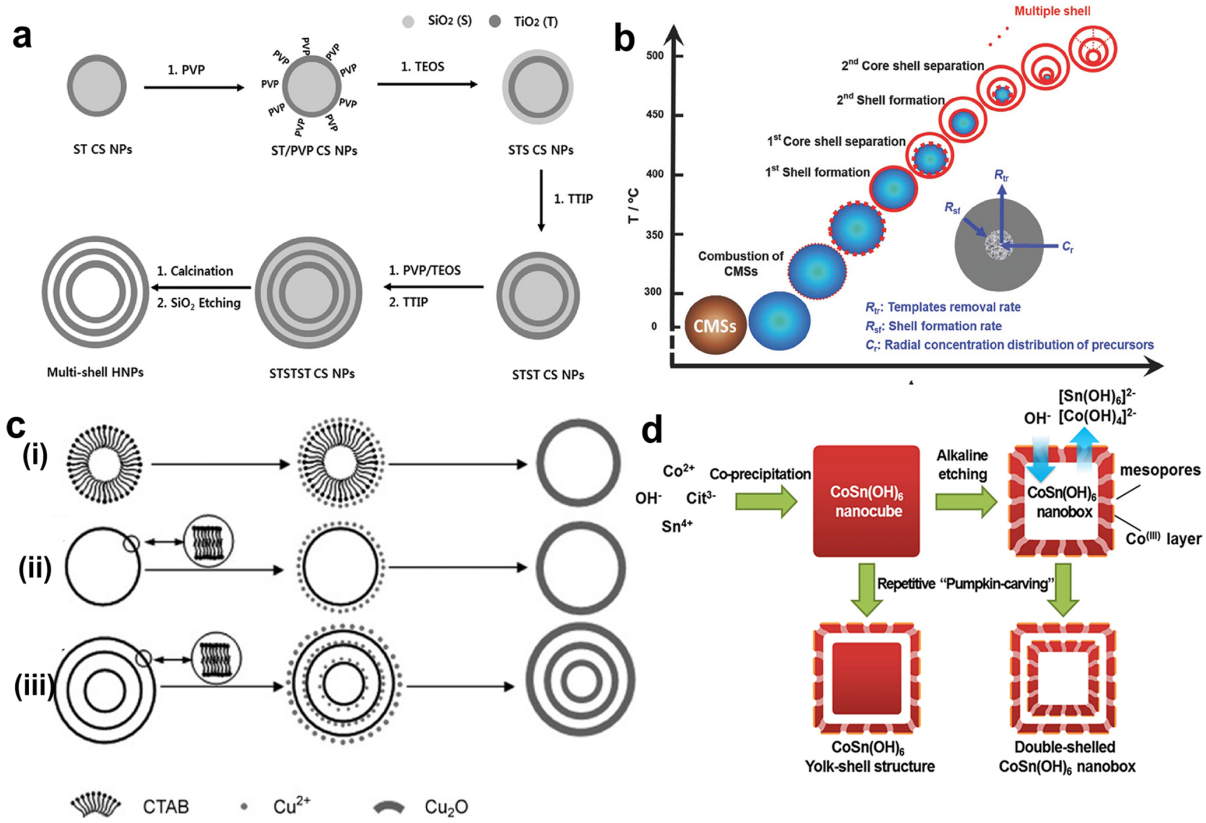


**Figure 5** (a) Schematic illustration of synthesis of $TiO_2$ TSHSs via hard-template method. Reproduced with permission from Ref. [78]. Copyright©2014, WILEY-VCH. (b) Illustration of the formation of HoMSs through STA. Reproduced with permission from Ref. [80]. Copyright©2018, WILEY-VCH. (c) Schematic illustration of the formation of different $Cu_2O$ hollow structures in the presence of a CTAB template: (i) micelle; (ii) single-lamellar vesicle; (iii) multilamellar vesicle. Reproduced with permission from Ref. [84]. Copyright©2007, WILEY-VCH. (d) Schematic illustration of the synthesis procedure for $CoSn(OH)_6$ hollow nanoboxes via self-template method. Reproduced with permission from Ref. [90]. Copyright©2013, Springer Nature.

critical threshold, micellar structures can form in solution and guide the growth of precursor species, ultimately yielding nanomaterials with defined structures. For instance, Xu *et al*. [84] employed hexadecyltrimethylammonium bromide (CTAB) as a soft template to synthesize novel hollow $Cu_2O$ nanostructures with the assistance of CTAB vesicles and multilamellar vesicles, as shown in Figure 5c. By tuning the CTAB concentration, $Cu_2O$ hollow spheres with different numbers of shells were successfully obtained. Yujii *et al*. [85] synthesized monodisperse hollow mesoporous organosilica using 1,2-bis(triethoxysilyl) ethane as the precursor and CTAB together with sodium dodecyl sulfate as soft templates. In another example, Liang *et al*. [86] reported a one-pot synthesis of hollow porous carbon spheres using alkali lignin extracted from corn stalks as the carbon precursor, CTAB as the soft template, $Zn^{2+}$ as a crosslinking agent, and $KHCO_3$ as an activating agent.

### *Self-template method*

The self-template method typically refers to a two-step synthesis strategy. First, a template is synthesized. Then, through physical or chemical changes, the template is directly converted into the shell of the hollow

structure or its precursor. This means that the template material is completely or partially integrated into the shell during the construction of the hollow nanostructure. Unlike the hard- and soft-template methods, in the self-template method, the template not only provides space for the formation of the internal cavity but also serves as the source material for constructing the shell [87]. This method offers advantages such as simplified procedures, facile controllability, and low production cost. According to the chemical principles, self-templating strategies can be classified into electrochemical replacement, the Kirkendall effect, Ostwald ripening, and chemical etching, etc.

Xiong *et al*. [88] used a mixture of cuprous oxide and polyvinylpyrrolidone (PVP) as the precursor solid and exploited the capacity of ion-exchange reactions to construct HoMS. By appropriately controlling the precursor system and reaction kinetics, a series of anion-exchange reactions were achieved, resulting in the formation of single-, double-, triple-, and quadruple-shelled $Cu_2S$ hollow spheres.

Ostwald ripening can also facilitate the formation of hollow structures. Zhang *et al*. [89] reported a spontaneous hollowing phenomenon by dispersing solid silica spheres in an aqueous $NaBH_4$ solution, where all solid silica particles were transformed into hollow structures through a dissolution-regrowth process. The continued growth of the shell, accompanied by dissolution of the core, was attributed to Ostwald ripening. This self-templating strategy is extensible to a broad range of core-shell particle systems and shows considerable potential for applications in catalysis, drug delivery, and related fields.

In addition, hollow structures can be fabricated via chemical etching. Wang *et al*. [90] fabricated mesoporous single-crystal $CoSn(OH)_6$ hollow structures with multilevel interiors (Figure 5d). In this process, $Co^{2+}$ and $Sn^{4+}$ ions were rapidly co-precipitated to form solid single-crystalline $CoSn(OH)_6$ nanocubes. Sodium citrate was introduced as a growth modulator to regulate the crystallization process, ensuring uniform particle size and well-defined cubic morphology. Subsequently, self-templating chemical etching occurred under strongly alkaline conditions by using NaOH. By repeating the sequence of $CoSn(OH)_6$ regrowth followed by alkaline etching, a series of hollow architectures, including single-shelled hollow structures, yolk-shell structures, and HoMS, can be constructed.

## PHOTOTHERMAL-SYNERGISTIC ANTIBACTERIAL STRATEGIES BASED ON HOLLOW STRUCTURE

Although PTT has unique advantages, it still has limitations in terms of penetration depth, treatment accuracy, and potential thermal damage. To overcome these challenges and achieve more efficient and safer antibacterial treatment, photothermal-synergistic antibacterial strategies based on hollow structures have been investigated (Figure 6).

### Chemodynamic therapy synergy

CDT is an emerging antibacterial strategy that employs Fenton/Fenton-like metal nanocatalysts to convert hydrogen peroxide ($H_2O_2$) into hydroxyl radicals (•OH) for eliminating bacterial infections [91,92]. By integrating PTT with CDT, synergistically enhanced antibacterial efficacy can be achieved. First, the high temperature generated by PTT significantly accelerates the kinetics of Fenton/Fenton-like reactions, as in the

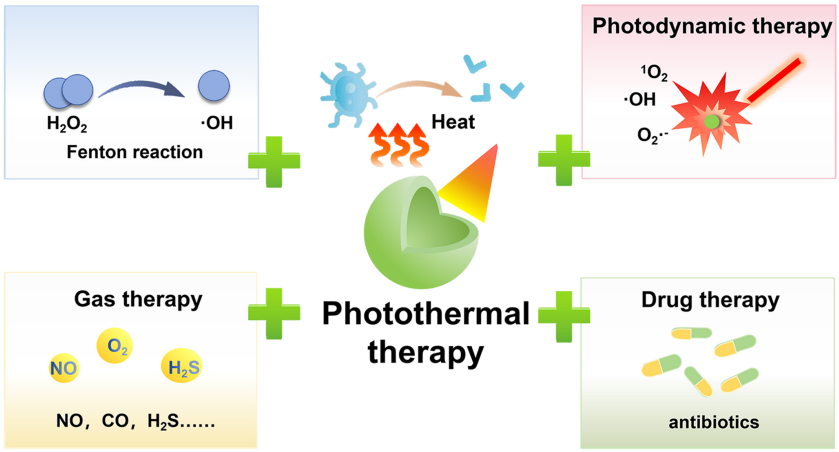


**Figure 6** Multiple photothermal synergistic therapy strategies based on hollow structures, including chemodynamic therapy synergy, photodynamic therapy synergy, gas therapy synergy and drug therapy synergy.

Arrhenius equation, the reaction rate increases exponentially with temperature, resulting in enhanced ROS production within a shorter timeframe. Second, the thermal effect can disrupt bacterial bioflims and increase their permeability, facilitating the entry of metal ions into the interior of bacteria and promoting intracellular Fenton/Fenton-like reactions. Third, the oxidative damage caused by ROS produced by CDT can further enhance the thermosensitivity of bacteria and aggravate the thermal damage caused by PTT. Therefore, the synergy between CDT and PTT is fundamentally mechanistic rather than additive.

Copper is one of the metal elements commonly found in natural enzyme active centers and is abundant and cost-effective, which has led to growing interest in copper-based nanozymes. Shi *et al*. [26] synthesized hollow mesoporous CuO nanozymes via a template-assisted method that simultaneously exhibits photothermal properties, peroxidase-like catalytic activity, and glutathione-depleting capability, as Figure 7a illustrated. Under light irradiation, photothermal heating contributed to bacterial killing, while efficient catalytic conversion of $H_2O_2$ into ROS further amplified antibacterial efficacy. This nanozyme platform integrating PTT and CDT provides a promising therapeutic strategy for clinical bacterial infections.

Hydrogels, which contain large amounts of water and exhibit excellent biocompatibility as well as the ability to maintain a moist wound environment, are advantageous carriers for antibacterial therapy. Incorporating hollow-structured photothermal nanoplatforms into hydrogels can improve the therapeutic outcomes for infected wounds. Liu *et al*. [93] embedded nanocomposites composed of PDA, hollow cerium dioxide, and montmorillonite into hydrogels, endowing them with outstanding photothermal performance and high nanozyme activity. The synergistic PTT and PDT exhibited effective antibacterial activity against both *E. coli* and *S. aureus*. In addition, the hydrogel promoted fibroblast proliferation and granulation tissue formation, thereby accelerating the healing of bacteria-infected wounds.

## Photodynamic therapy synergy

PDT involves the absorption of photons by photosensitizers under light irradiation, followed by the excitation of electrons and subsequent energy transfer to molecular oxygen to generate ROS, which induce cellular

damage and therapeutic effects [94]. The combination of PTT and PDT can achieve synergistic antibacterial efficacy through multiple mechanisms. On the same hollow structured platform, PDT and PTT can share light excitation, enabling the simultaneous conversion of light energy into heat and ROS, promoting the efficiency of treatment. The local hyperthermia generated by PTT can destroy the structure of bacterial biofilms and loosen the extracellular polymeric substance matrix, which facilitates the penetration of photosensitizers into deeper biofilm layers, therefore amplifying PDT efficacy. Moreover, mild PTT may downregulate bacterial heat-shock proteins, thereby weakening stress-protection pathways and increasing bacterial susceptibility to PDT-generated ROS.

Chlorin e6 (Ce6), a photosensitizer derived from natural chlorophyll, has attracted considerable attention owing to its well-defined molecular structure, low toxicity, and strong photodynamic activity. Lin *et al*. [95] immobilized Ce6 molecules onto hollow Ag-Au nanoparticles, enabling both photothermal responses and ROS generation under near-infrared (NIR) irradiation (Figure 7b). Through the synergistic combination of PTT and PDT, these nanoparticles effectively eliminated both planktonic and surface-adhered bacteria at wound sites and promoted epithelial cell migration and angiogenesis, thereby accelerating wound healing.

The formation of Schottky junctions can further enhance charge separation efficiency and promote greater ROS generation by photosensitizers under light irradiation. Wang *et al*. [96] prepared Au@$Bi_2S_3$ core-shell nanostructures via a hard-template approach combined with a polyol method. These nanoparticles exhibited strong NIR light absorption and typical Schottky junction behavior, which enhanced the separation efficiency of NIR-induced electron-hole pairs and resulted in substantial ROS generation. Consequently, rapid and precise antibacterial activity was achieved through combined PTT and PDT effects.

## Drug therapy synergy

The antibacterial efficacy of standalone PTT is inherently temperature dependent. To further enhance therapeutic outcomes, antimicrobial or bactericidal agents are frequently combined with PTT. Depending on the type and severity of infectious diseases, appropriate antibacterial drugs can be selectively incorporated to achieve optimized treatment effects. The synergistic mechanisms between drug therapy and PTT are primarily reflected in three aspects. First, antibacterial agents are often loaded into hollow structures, where the local heat generated by PTT enables thermoresponsive drug release and promotes drug diffusion. Second, the localized temperature increase induced by PTT enhances bacterial membrane permeability, facilitating drug entry into bacteria and thereby improving bactericidal efficacy. Third, drug therapy compensates for the limitations of PTT alone by eliminating bacteria that are not completely inactivated by photothermal treatment.

Ciprofloxacin is an organic compound with broad-spectrum antibacterial activity and has been shown to inhibit *E. coli*, *S. aureus* and other pathogens. Gao *et al*. [97] prepared hollow polydopamine microspheres loaded with ciprofloxacin. Upon NIR irradiation, the photothermal response of polydopamine triggered controlled release of the antibacterial agent, resulting in effective suppression of bacterial infection and promotion of wound healing.

Linalool is a naturally derived antibacterial agent extracted from various essential oils and exhibits excellent antimicrobial activity against a wide range of pathogens. Wang *et al*. [98] synthesized $Bi_2S_3$ hollow microspheres via a hard-template-assisted method, as the Figure 7c shown. A phase-change material,

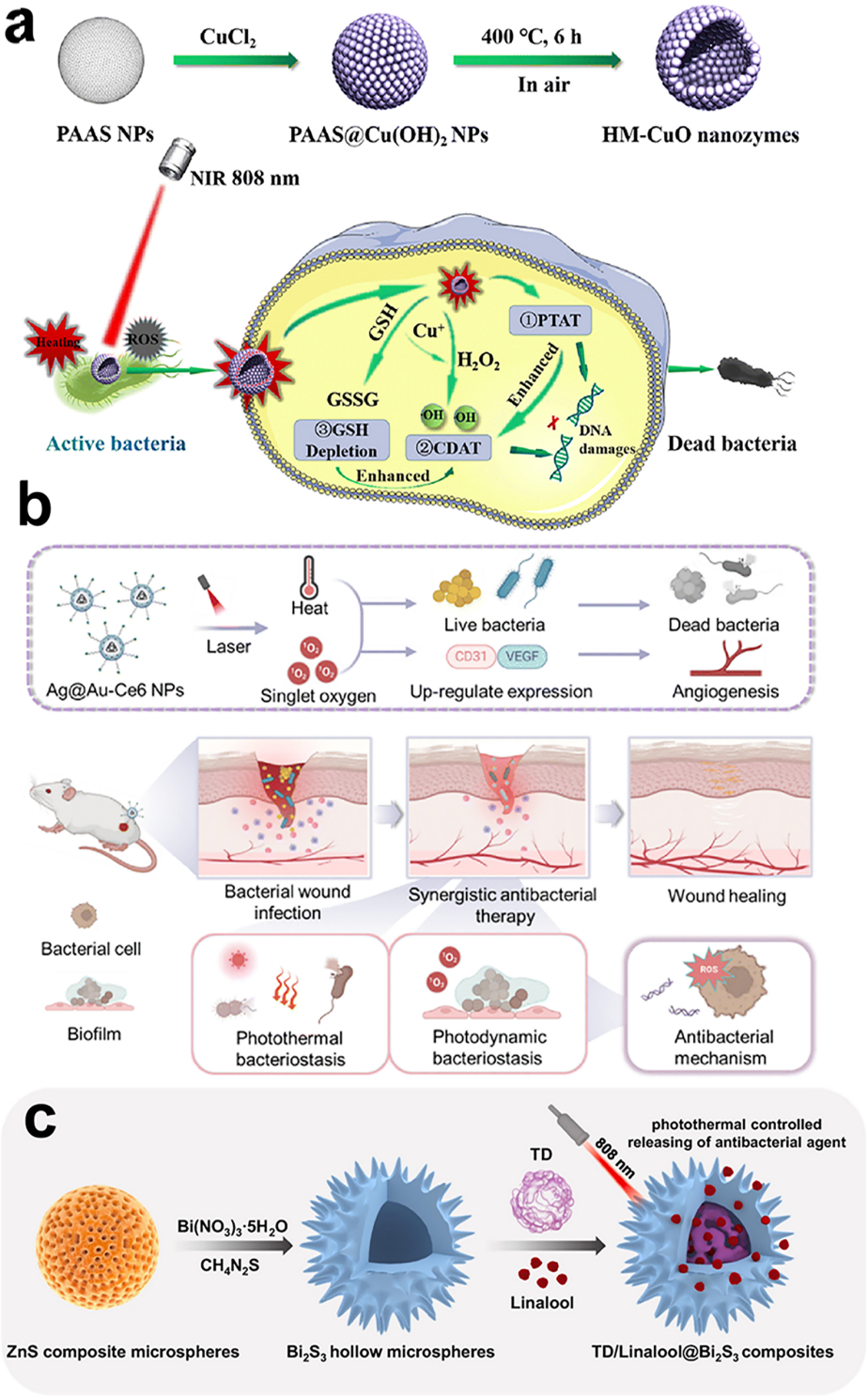


**Figure 7** (a) Schematic illustration of the synthetic process of HM-CuO nanozymes for photothermal-reinforced catalytic antibacterial therapy. Reproduced with permission from Ref. [26]. Copyright©2022, Royal Society of Chemistry. (b) Schematic illustration of Ag@Au-Ce6 NPs for bacterial eradication and wound healing acceleration. Reproduced with permission from Ref. [95]. Copyright©2023, Royal Society of Chemistry. (c) Schematic illustration of the construction of the TD/Linalool@$Bi_2S_3$ composite nanostructures. Reproduced with permission from Ref. [98]. Copyright©2019, Elsevier B.V.

tetradecanol, was subsequently employed to encapsulate linalool within the hollow interior. Under NIR irradiation, $Bi_2S_3$ generated localized photothermal heating, which induced melting of the phase-change material and subsequent release of the antibacterial agent. Through the synergistic effects of PTT and drug therapy, both Gram-negative and Gram-positive bacteria were effectively eradicated.

## Gas therapy synergy

When applied to specific disease conditions, PTT may be limited by factors such as tissue hypoxia and upregulation of heat-shock proteins. Various gas molecules, including nitric oxide (NO), carbon monoxide (CO), and hydrogen sulfide ($H_2S$), possess unique biological functions and play important roles in pathological processes [99–101]. These gases have low molecular weights, allowing them to freely diffuse through biofilms to exert antibacterial effects inside bacteria or biofilms, while also mediating critical physiological processes such as vascular regulation and immune cell activity. Synergizing PTT with gas therapy can overcome the limitations of hyperthermia alone. First, in gas therapy systems, hollow-structured platforms are commonly used to load gases, gas precursors, or gas donors. The photothermal effect generated by PTT can trigger gas release by accelerating donor decomposition or through heat-responsive activation. Second, the hyperthermia produced by PTT can increase bacterial membrane permeability, damage membrane proteins, and loosen the EPS matrix, thereby facilitating the penetration of gaseous molecules into deeper regions of biofilms and enhancing their therapeutic efficacy. Third, different gases possess distinct biological functions and can work synergistically with PTT to achieve improved therapeutic outcomes. For example, gaseous molecules such as NO and CO can directly damage bacterial components through nitrosative or oxidative stress, thereby complementing the thermal ablation effect of PTT. Moreover, NO has been shown to suppress the expression of heat-shock proteins (HSPs), thereby reducing bacterial thermotolerance and increasing bacterial susceptibility to photothermal damage [102,103]. Consequently, Synergizing PTT with gas therapy has emerged as an effective strategy to overcome the limitations of standalone PTT.

CO is a multifunctional signaling molecule that has been shown to promote vasodilation, exert anti-inflammatory effects, and possess antibacterial activity in biological systems [104]. Lv *et al*. [105] synthesized hollow bismuth nanospheres loaded with hexaaminolevulinic acid hydrochloride (HAL) and incorporated them into a dual-crosslinked hydrogel. Under NIR irradiation, bismuth nanoparticles generated photothermal effects while gradually releasing HAL, which was metabolized to produce CO and bilirubin, thereby enhancing antibacterial and anti-inflammatory responses. This hydrogel platform achieved synergistic antibacterial effects through PTT and gas therapy, providing an effective solution for infected wound healing.

NO is crucial for normal wound healing, participating in the regulation of multiple processes including inflammatory response, antibacterial action, cell proliferation, and angiogenesis [106,107]. Rouillard *et al*. [108] developed NO-releasing chitosan oligosaccharides (COS/NO) as alternatives to conventional antibiotics. As illustrated in Figure 8a, the NO produced by this platform is further converted into species such as NO•, $NO_2$•, $N_2O_2$ and $ONOO^-$, which damage bacterial cell membranes through nitrosative and oxidative stress. The results indicate that nitric oxide exhibits broad-spectrum antibacterial properties and can enhance the efficacy of conventional antibiotics when used in sequential combination with them.

Moreover, during the inflammatory phase, NO participates in immune regulation and exhibits broad-

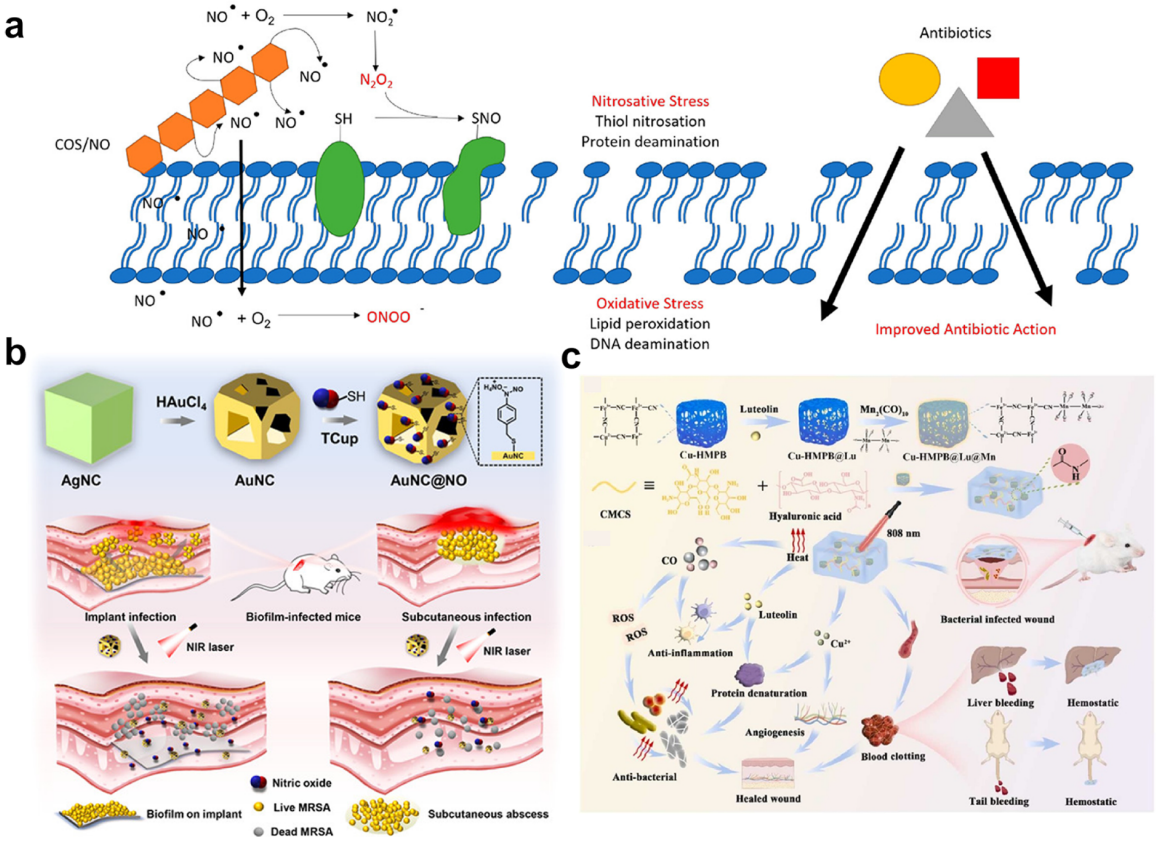


**Figure 8** (a) Scheme depicting the antibacterial effect of COS/NO. Reproduced with permission from Ref. [108]. Copyright©2020, American Chemical Society. (b) Illustration of the synthesis of AuNC@NO and its application in biofilm infection. Reproduced with permission from Ref. [109]. Copyright©2021, American Chemical Society. (c) Scheme of the synthesis of smart response CO hydrogel and its application in biofilm infection. Reproduced with permission from Ref. [111]. Copyright©2025, Elsevier B.V.

spectrum antibacterial activity; during the proliferative phase, it promotes fibroblast migration and proliferation as well as neovascularization. Therefore, supplementing NO at wound sites is a promising therapeutic strategy. Tang *et al*. [109] reported a nitrate-releasing hollow gold nanocage (AuNC@NO) that can release nitric oxide (NO) under NIR irradiation and generate hyperthermia for biofilm eradication (Figure 8b). AuNC@NO was prepared by immobilizing a temperature-responsive NO donor onto gold nanocages (AuNCs) via thiol-gold interactions. AuNC@NO exhibits excellent photothermal conversion stability, slowly releases NO at physiological temperature, and rapidly releases NO on−demand under NIR irradiation. The synergy between NO gas therapy and PTT enables AuNC@NO to achieve a 4-log reduction in bacteria and 85.4% biofilm removal under NIR light. The AuNC@NO nanocomposite developed in this study offers a useful PTT−combined gas therapy strategy for the treatment of biofilm-associated infections.

## Multimodal synergistic platforms

To achieve superior therapeutic efficacy, multiple treatment modalities are often integrated with PTT to construct multimodal synergistic platforms. Qi *et al*. [110] fabricated core-shell nanostructures composed of gold nanorods and mesoporous silica, which were co-loaded with ICG and S-nitrosothiols. Under NIR

irradiation, Au generates a photothermal response that induces localized temperature elevation, while ICG generates ROS, enabling antibacterial activity through PTT and PDT. Thermal stimulation triggers the release of NO from the loaded S-nitrosothiols, thereby exerting anti-inflammatory effects. Through the synergistic integration of PTT, PDT and gas therapy, this nanoplatform effectively disrupted pathogenic bacterial biofilms and exhibited potent antibacterial activity, providing a promising solution for the clinical management of periodontitis.

In another study, Cao *et al*. [111] synthesized copper-doped hollow mesoporous Prussian blue nanoparticles (Cu–HMPB NPs), loaded them with luteolin, and covalently conjugated them with the temperature–sensitive CO donor $Mn_2(CO)_{10}$ (Figure 8c). Using a crosslinking agent, these nanoparticles were incorporated into a hydrogel. Under NIR irradiation, the hydrogel demonstrated excellent photothermal performance and enabled on–demand release of CO gas. The CO gas effectively penetrated mature biofilms and disrupted their extracellular polymeric substance, which enhanced the penetration of the biofilm inhibitor luteolin and prevented secondary biofilm formation by planktonic bacteria. Luteolin also exhibited effective antioxidant properties. Overall, the synergy of gas therapy, drug therapy, and PTT shows high potential in addressing clinical challenges caused by biofilm infections.

In addition to these representative combinations in Figure 6, other therapeutic modalities such as sonodynamic therapy and immunomodulation may also serve as promising partners for hollow-structured photothermal antibacterial platforms. Sonodynamic therapy (SDT) is a non-invasive treatment method, which refers to the process where the sonosensitizer generates ROS under specific frequencies and intensities of ultrasound, killing bacteria or other microorganisms [112,113]. SDT can overcome the limited penetration depth of PTT, making it a promising approach for the treatment of deep-seated infections. Immunotherapy refers to strategies that activate or enhance the patient's own immune system, enabling it to recognize and attack disease [114]. When combined with PTT, it may integrate high-temperature physical ablation with immune-memory-related effects. Accordingly, these two modalities are briefly highlighted here as emerging extensions of hollow-structured photothermal synergistic antibacterial system.

## APPLICATIONS OF HOLLOW-STRUCTURED PHOTOTHERMAL ANTIBACTERIAL THERAPY IN DISEASE TREATMENT

This section first outlines the strategy–scenario matching principles that govern the selection of photothermal synergistic therapies in different infection settings. It then summarizes the representative applications of hollow-structured photothermal antibacterial platforms in various disease scenarios, highlighting how pathological characteristics determine the choice of appropriate synergistic strategies.

### Strategy-scenario matching principles

The selection of photothermal synergistic strategies is dictated by the pathological characteristics of different infection scenarios. The first factor is the depth of infection. For superficial infections such as open wounds or cutaneous surface infections, light can easily reach the lesion, and local oxygen supply is relatively adequate. In such cases, PTT can rapidly achieve thermal sterilization and biofilm disruption. PDT can be

employed in combination, producing ROS to further amplify the antimicrobial effect, thereby creating synergy between thermal effects and oxidative damage [115]. For deep-seated infections, PTT alone is limited by the penetration depth of light and the diffusion range of heat, making it difficult to reach the deep lesion location [116]. In contrast, gas molecules, characterized by their small molecular weight and strong diffusion capability, can more efficiently penetrate biofilm matrices and reach areas where thermal therapy alone is insufficient. Therefore, PTT combined with gas therapy is generally better suited for deep-seated infections.

The microenvironment at the infection site also significantly influences the selection of photothermal synergistic strategies. For instance, in diabetic wound infections, the microenvironment is often characterized by high $H_2O_2$ levels, low pH, and persistent inflammation [117]. In these cases, CDT can be combined with PTT, where CDT converts endogenous $H_2O_2$ into •OH, and the localized hyperthermia generated by PTT further enhances the Fenton or Fenton-like reaction, achieving synergistic antimicrobial effects [118]. In hypoxic infection sites, the efficacy of PDT is compromised by insufficient oxygen supply, while CDT can serve as an alternative to PDT in combination with PTT.

When temporal and spatial controllability is required for bacterial infection treatment, such as in implant-associated infections that demand long-term antimicrobial activity, drug therapy combined with PTT offers superior adaptability. Hollow structures loaded with drugs can leverage PTT to enable controlled and sustained drug release, while PTT enhances bacterial membrane permeability and improves drug penetration, resulting in potent bactericidal effects.

Based on this, this section presents recent advances in hollow-structured photothermal antibacterial materials according to different application scenarios, including cutaneous and soft tissue infections, ocular infections, oral infections, and other deep-seated infections.

## Cutaneous and soft tissue infections

Cutaneous and soft tissue infections are typically characterized by high local accessibility, convenient exogenous light irradiation, and ease of topical drug administration. The therapeutic requirements for such infections encompass not only rapid sterilization but also biofilm disruption, inflammation control, and tissue repair.

### *Superficial wound infections*

Superficial wound infections refer to a localized inflammatory response caused by the excessive growth and invasion of microorganisms following trauma or surgery involving the epidermis and dermis of the skin. The infection is confined to the skin and subcutaneous tissues and does not extend into deeper tissues such as muscles or body cavities. However, if improperly managed, superficial wound infection may spread to deeper tissues, leading to more severe deep tissue infections and threatening people's health. For superficial wound infections, due to the exposed nature of the lesion and the high accessibility of external light, PTT is more suitable for being combined with PDT, silver ion release, or local drug dressings to achieve efficient sterilization within a shorter period of time.

Silver nanoparticles are a class of antibacterial agents that can penetrate bacterial cell walls and disrupt

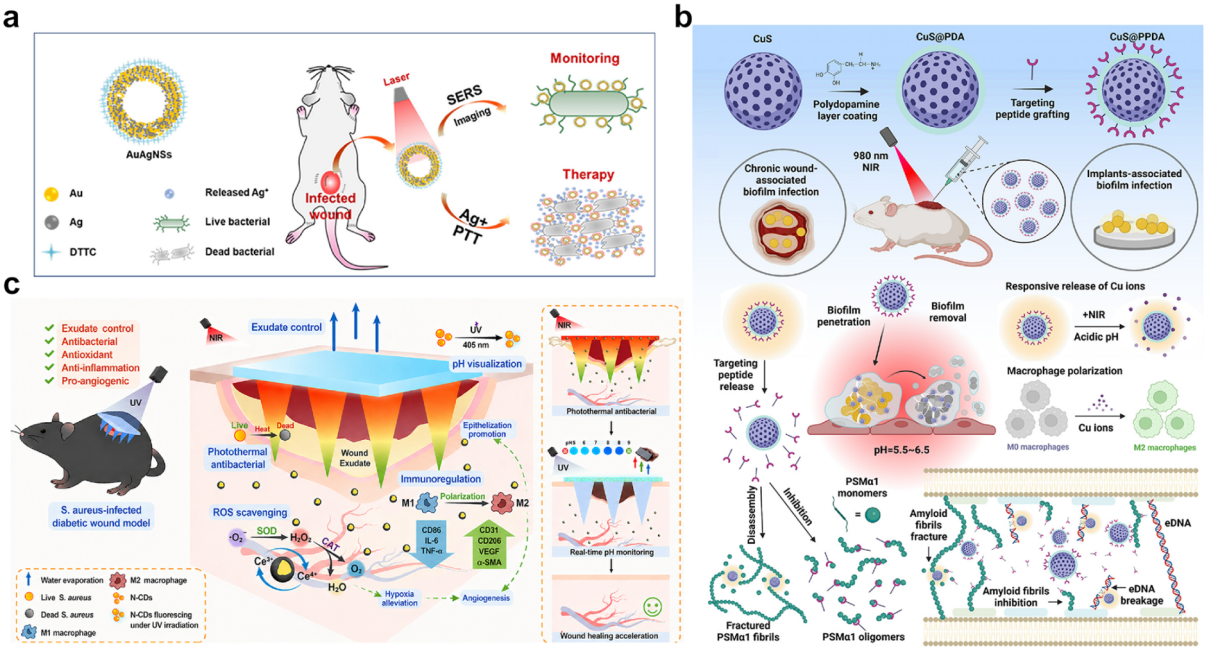


**Figure 9** (a) Scheme of Raman tag 3,3′-diethylthiatricarbocyanine iodide (DTTC)-conjugated gold-silver nanoshells (AuAgNSs) and application in infected wound. Reproduced with permission from Ref. [121]. Copyright©2020, Elsevier Ltd. (b) Fabrication of PSMα1-targeting photothermal nanoplatform and its underlying mechanism for the therapeutics of biofilm-associated infections. Reproduced with permission from Ref. [125]. Copyright©2025, American Chemical Society. (c) Schematic for infected diabetic wound management mechanism using the GM/P@C/CDs MN. Reproduced with permission from Ref. [127]. Copyright©2025, American Chemical Society.

bacterial growth and proliferation [119,120]. However, their photothermal efficiency is inferior to that of gold nanoparticles. To address this limitation, He *et al*. [121] developed hollow Au-Ag core-shell nanoparticles (Figure 9a). In a murine model of chronic methicillin-resistant *S. aureus* (MRSA)-infected wounds, this nanoplatform exhibited pronounced photothermal responses under NIR laser irradiation, generating high temperatures to kill bacteria while releasing silver ions. It effectively inhibited bacterial infection, promoted wound healing, and demonstrated very low toxicity. The results indicate that this nanoplatform holds strong potential for clinical translation as an antibacterial therapeutic agent.

Waterborne polyurethane (WPU) is an aqueous dispersion that provides a favorable environment for the stability and uniform distribution of photothermal hollow nanoparticles and exhibits excellent biocompatibility. Consequently, WPU-based wound dressings have attracted considerable attention. Salehi *et al*. [122] developed a multifunctional WPU-based wound dressing incorporating polydopamine-coated ZnO core-shell nanoparticles decorated with surface-modified silver nanoparticles (ZnO@PDA/Ag). Under NIR irradiation, the WPU film displayed efficient photothermal conversion and the ability to generate singlet oxygen. The results demonstrated that, through NIR-triggered synergistic PTT and PDT therapy, the WPU film achieved complete inhibition of both *E. coli* and *S. aureus*, indicating significant potential for superficial wound management.

### *Diabetic wound infections*

Diabetic wound infections are often accompanied by persistent bacterial biofilms, chronic inflammation,

hyperglycemia, oxidative stress, and impaired angiogenesis, all of which greatly hinder effective treatment [117]. Among these factors, biofilm formation represents a major barrier. Because the dense EPS matrix restricts the diffusion of therapeutic agents, the negatively charged biofilm surface limits the adhesion of many nanoplatforms, and the interior of the biofilm often exhibits an acidic, hypoxic, and heterogeneous microenvironment [123]. These features not only reduce the efficacy of conventional antibacterial agents but also weaken the performance of standalone PTT. In this context, hollow-structured photothermal platforms are advantageous for diabetic wound infections. Photothermal heating can loosen the EPS matrix, reduce biofilm cohesion, and increase bacterial membrane permeability, which can facilitate the penetration of drugs, catalytic species, or gaseous molecules into deeper biofilmgions [124]. In addition, structural modifications can be made to hollow-structured photothermal synergistic antibacterial nanoplatforms to enhance their biofilm-targeting capability. Charge-regulating strategies, cationic surface modification, and peptide/ligand functionalization can improve the local adhesion and accumulation of nanoplatforms on negatively charged biofilms. Moreover, pH-responsive or enzyme-responsive release systems can further exploit the pathological microenvironment of diabetic wounds to achieve efficient therapeutic delivery. Therefore, the treatment of diabetic wound infections is suitable for hollow photothermal platforms that integrate biofilm disruption, responsive release, and multifunctional synergistic therapy.

Chen *et al*. [125] conjugated the KG7 peptide onto polydopamine-modified hollow copper sulfide (CuS) nanoparticles to construct a biofilm-targeting photothermal nanoplatform (CuS@PDA) (Figure 9b). Through the synergistic effects of KG7-mediated biofilm inhibition and PTT, a biofilm inhibition rate of 94.7% was achieved, significantly accelerating diabetic wound healing.

In addition to antibacterial activity, regulation of glucose levels within the diabetic wound microenvironment is also critical. Wang *et al*. [126] synthesized hollow mesoporous molybdenum single-atom nanozymes encapsulating glucose oxidase. Upon NIR irradiation, photothermal conversion was induced while simultaneously promoting the release of glucose oxidase, thereby accelerating the conversion of glucose to gluconic acid. This process reduced local glucose concentration and pH, enhancing the conversion of hydrogen peroxide (generated by nanozyme catalysis) into hydroxyl radicals for improved antibacterial efficacy. This work introduces a novel strategy for diabetic infection treatment by integrating NIR responsiveness, cascade-triggered antibacterial activity, and glucose regulation.

Hydrogel microneedles exhibit excellent biocompatibility, tunable mechanical properties, and swelling-triggered sustained drug release behavior, making them well-suited for integration with photothermal hollow structures in diabetic wound treatment. Shi *et al*. [127] developed a multifunctional hydrogel microneedle patch composed of methacrylated gelatin, polydopamine-coated cerium oxide core-shell structures, and nitrogen-doped carbon quantum dots (N-CDs) (Figure 9c). Under NIR irradiation, the photothermal response of polydopamine balanced hydrogel swelling and water evaporation, achieving localized antibacterial effects and exudate management. Meanwhile, N-CDs exhibited pH-responsive fluorescence changes, allowing real-time pH monitoring during the critical early stages of wound healing. The cerium oxide nanozyme displayed superoxide dismutase and catalase-like activities, scavenging ROS, alleviating hypoxia, and promoting angiogenesis. The hydrogel microneedle patch achieved 99.9% wound closure, demonstrated potent antibacterial activity, and integrated gradient photothermal therapy, exudate management, and pH monitoring, offering an effective strategy for diabetic wound treatment.

### *Skin abscesses*

Skin abscesses are infectious soft tissue diseases characterized by localized accumulation of pus and can arise from bacterial infection or trauma. In addition to causing direct skin damage, abscesses may lead to secondary skin disorders or recurrent infections. Skin abscesses have characteristics such as local swelling, accumulation of pus, and clear biological membrane barriers. Therefore, a microneedle-mediated local delivery strategy is more suitable, combined with mild PTT and antibacterial drugs to synergize, to improve lesion penetration, reduce recurrence, and control inflammation. Jin *et al*. [128] designed a dissolvable microneedle patch encapsulating photothermal core-shell Au@ZnO/Ce nanoparticles (AZC) and vancomycin (Figure 10a). The sharp microneedle tips readily penetrated the skin barrier and bacterial biofilms, enabling effective delivery of AZC and vancomycin to infection sites. Through mild photothermal therapy (⩽42 °C) and the antibacterial action of vancomycin, effective bacterial clearance and synergistic treatment of abscesses were achieved. Moreover, sustained synergistic release of cerium ions ($Ce^{3+}$/$Ce^{4+}$) and zinc ions ($Zn^{2+}$) significantly alleviated oxidative stress, reduced inflammation, and promoted tissue regeneration. This multifunctional microneedle patch with potent antibacterial and anti-inflammatory activities provides an effective strategy for skin abscess treatment.

## Ocular infections

The challenge in treating ocular infections lies in the rapid progression of the infection, along with the extremely fragile nature of the eye tissues, which have limited tolerance to thermal damage and long-term drug stimulation. Therefore, more efficient and controllable photothermal synergy strategies are required.

### *Bacterial keratitis*

Bacterial keratitis (BK) is an infection of corneal tissue caused by various bacteria. It is an ocular surface infection that progresses rapidly, threatens vision, and can leave irreversible visual sequelae, posing a significant threat to human health [129,130]. Over the past few decades, the global number of contact lens wearers has increased rapidly, leading to a corresponding rise in the proportion of bacterial keratitis cases [131]. Clinical treatment for BK typically involves topical application of fluoroquinolone antibiotics. However, antibiotic misuse and the formation of bacterial biofilms in ocular infections have led to increasingly serious bacterial resistance problems [132]. Therefore, there is an urgent need for novel methods capable of effectively clearing bacterial biofilms to treat BK. BK progresses rapidly, and corneal tissue is highly sensitive to heat damage. Therefore, synergistic strategies combining PTT with PDT or CDT are more suitable. These approaches disrupt the biofilm barrier through mild hyperthermia and achieve efficient sterilization via sustained ROS generation, thereby avoiding thermal damage to tissues. Kong *et al*. [133] synthesized iron-cobalt oxide nanoparticles ($FeCoO_x$ NPs) with a double-shelled hollow structure via a self-templating method. As shown in Figure 10b, owing to their unique dual-shelled hollow structure and multivalent bimetallic characteristics ($Fe^{2+}$/$Fe^{3+}$ and $Co^{2+}$/$Co^{3+}$), the nanoparticle exhibited integrated photothermal, photodynamic, and oxidase-like (OXD) activities. Under NIR irradiation, the nanoparticles generated localized high temperatures through photothermal conversion, directly disrupting biofilms.

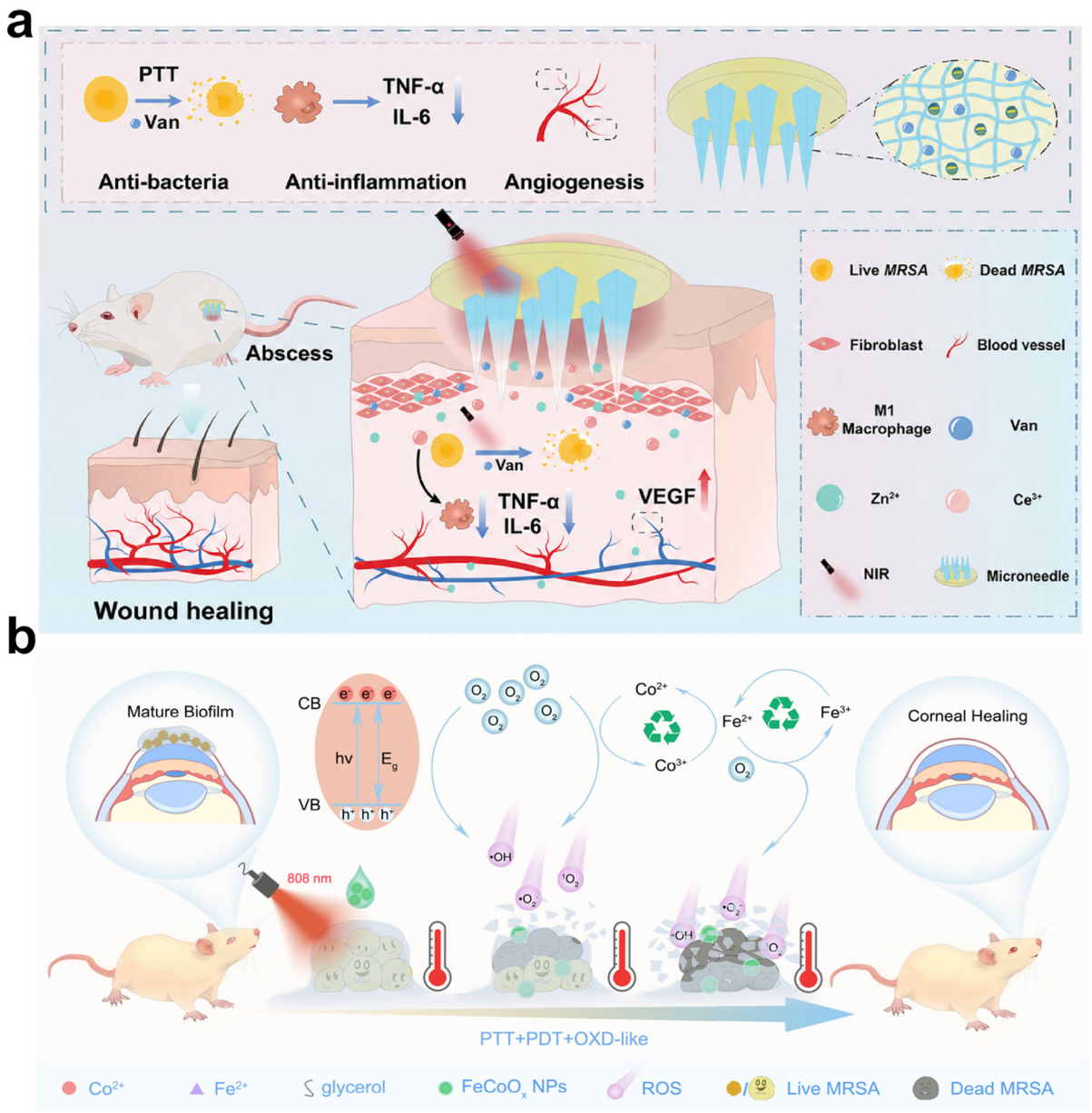


**Figure 10** (a) Schematic illustration of AZC/Van@MN promotes abscess wound healing through the integration of multiple mechanisms including bacterial clearance, anti-inflammatory response, and the promotion of angiogenesis. Reproduced with permission from Ref. [128]. Copyright©2025, Wiley-VCH. (b) Schematic illustration of the $FeCoO_x$ nanozymatic antibacterial agents for PTT/PDT/nanozymatic synergetic treatment of BK caused by MRSA infection. Reproduced with permission from Ref. [133]. Copyright©2025, Elsevier B.V.

Furthermore, under light, the nanoparticles produced a large amount of ROS, causing multiple oxidative damages to bacterial biomolecules. The dynamic cycle between $Fe^{2+}/Fe^{3+}$ and $Co^{2+}/Co^{3+}$ enabled the continuous generation of ROS *in vivo*, thereby constantly renewing catalytic sites and sustaining the persistent production of ROS, further damaging bacteria. As a result, a bactericidal efficiency of 99.97% against MRSA was achieved. Both *in vitro* and *in vivo* studies further confirmed that these multifunctional nanozymes not only disrupted preformed biofilms (clearance rate of 84.83%) but also inhibited biofilm regeneration (in-

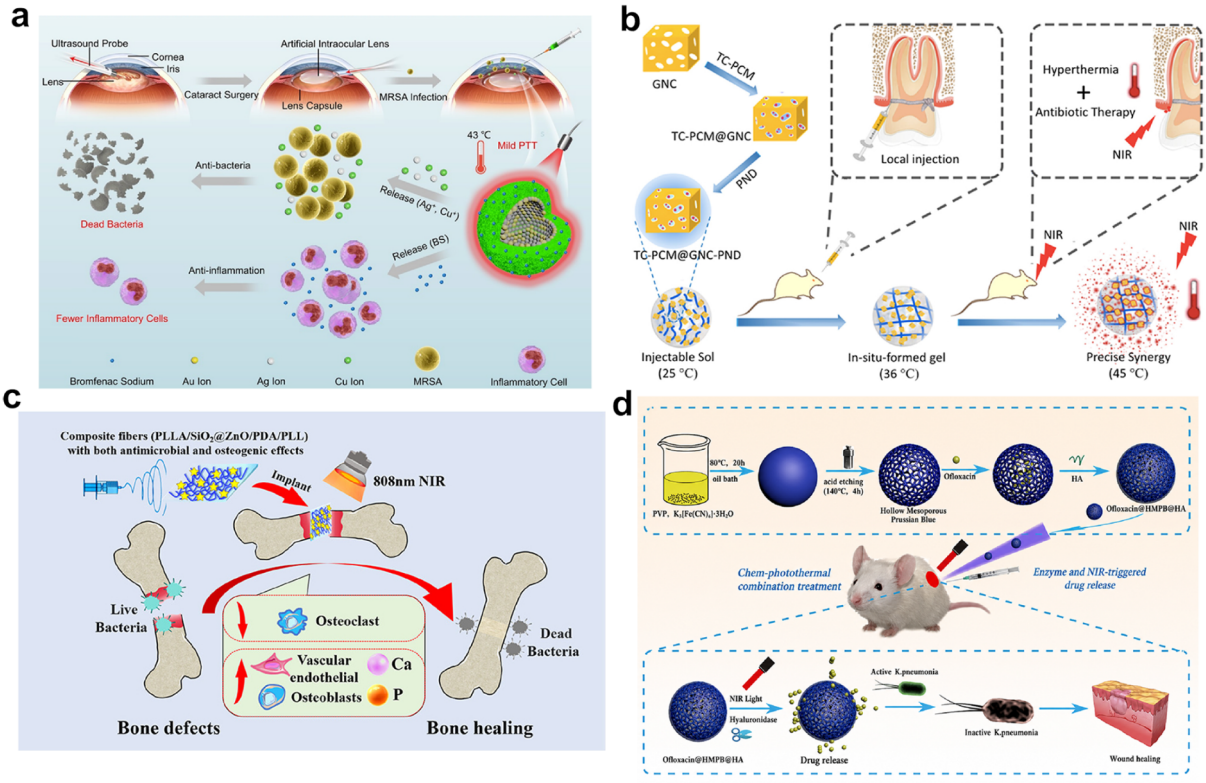


**Figure 11** (a) The schematic illustration of $AuAgCu_2O$-BS NPs for the treatment of endophthalmitis after cataract surgery. Reproduced with permission from Ref. [138]. Copyright©2020, The Author(s). (b) Schematic illustration of TC-PCM@GNC-PND as a combined platform for hyperthermia and antibiotics with an obvious synergistic antibacterial effect. Reproduced with permission from Ref. [140]. Copyright©2020, American Chemical Society. (c) The scheme of $SiO_2$-Coated ZnO for photothermal and photodynamic antibacterial applications in bone repair. Reproduced with permission from Ref. [150]. Copyright©2025, American Chemical Society. (d) Synthesis process of Ofloxacin@HMPB@HA NPs and its application for wound healing. Reproduced with permission from Ref. [155]. Copyright©2022, Wiley-VCH.

hibition rate of 85.43%). This research holds strong potential for clinical therapeutic applications in treating BK.

### *Endophthalmitis*

Endophthalmitis is a severe deep-seated infection occurring within the eyeball and is a common complication following cataract surgery [134,135]. In severe cases, it can lead to intensified inflammation, globe perforation, or even blindness [136]. Most cases arise from bacterial entry into the eye during surgery or trauma [137], underscoring the urgent need for rapid and effective antibacterial treatments. Ye *et al*. [138] synthesized hollow Au-Ag nanoparticles coated with a cuprous oxide shell via a template-assisted method and loaded the anti-inflammatory drug bromfenac sodium through pore adsorption (Figure 11a). *In vitro* studies demonstrated that under NIR irradiation, mild photothermal effects were generated, accompanied by $Ag^+$ and $Cu^+$ release and ROS production, resulting in efficient bacterial killing. The release of bromfenac sodium alleviated intraocular inflammation and promoted tissue recovery. Therapeutic efficacy was further confirmed in a rabbit post-cataract endophthalmitis model, indicating that this nanoplatform offers a promising

synergistic strategy for postoperative endophthalmitis treatment.

## Oral infections

The oral cavity consists of multiple components, including teeth, gums, tongue, palate, and salivary glands, and harbors a rich diversity of microorganisms. Bacteria and fungi commonly colonize tooth surfaces and periodontal tissues in the form of biofilms. Major oral infections include periodontitis and dental caries. Oral infections are a typical biofilm-driven disease, which are more suitable for treatment using PTT in combination with drug release, gas therapy, or multimodal strategies to eradicate bacterial biofilms and reduce the risk of local recurrence.

### *Periodontitis*

Periodontitis is a prevalent chronic inflammatory disease [139] primarily caused by the destruction of periodontal tissues by bacteria in dental plaque. Therefore, developing effective antibacterial strategies to combat periodontitis is crucial. Zhang *et al*. [140] combined hollow gold nanocages with a phase-change material and a thermosensitive copolymer and loaded tetracycline into the nanocages for periodontitis treatment (Figure 11b). Under NIR irradiation, the gold nanocages performed photothermal conversion, and the interaction between the phase-change material and thermosensitive polymer enabled the precise controlled release of tetracycline, achieving highly efficient bacterial clearance both in vitro and in a periodontitis model. Li *et al*. [141] designed $Fe_3O_4$@ZnO core-shell nanoparticles with ε-poly-*L*-lysine adsorbed onto the surface via electrostatic interactions. The $Fe_3O_4$ core imparted strong photothermal properties, ZnO contributed to biofilm disruption, and ε-poly-*L*-lysine, a natural cationic polypeptide, rapidly adsorbed onto negatively charged bacterial surfaces, enhancing nanoparticle adhesion and penetration. Combined with NIR irradiation, this nanoplatform effectively eliminated Porphyromonas gingivalis, accelerated periodontal wound healing, and prevented potential periodontal tissue damage.

### *Dental caries*

Dental caries is one of the most common chronic diseases worldwide and can lead to tooth pain, decay, and pulp infection, affecting individuals of all ages. Caries formation is primarily driven by cariogenic bacteria that dominate the oral microbiota and produce large amounts of lactic acid from fermentable carbohydrates, leading to enamel demineralization once the pH falls below a critical threshold [142]. Owing to its deep penetration and non-invasive nature, photothermal therapy shows considerable potential for caries treatment. Xu *et al*. [143] sequentially coated $Fe_3O_4$ nanoparticles with PDA, Ag, and glycol chitosan to construct a core-shell photothermal nanoplatform. Under NIR irradiation, polydopamine generated photothermal effects, while $Ag^+$ release further enhanced antibacterial activity, followed by magnetic removal of the nanoparticles. The nanoplatform effectively inhibited biofilm formation and exhibited excellent antibacterial activity against Streptococcus mutans, suggesting its potential as a photothermal therapeutic approach for dental caries and other open infectious wounds.

## Other deep-seated infections

Deep-seated infections occur in relatively enclosed regions of the body, such as internal cavities or organs. Compared with superficial infections, deep-seated infections are often concealed, difficult to detect, and associated with higher risks. The core challenges of deep-seated infections are limited light penetration, a restricted radius of thermal action, a closed lesion site, and often concomitant hypoxia. PTT is better suited for combination with gas therapy or responsive drug release strategies, leveraging the deep diffusion capability of gases or small molecules to compensate for the limitations of PTT alone. Additionally, cascade CDT is suited for lesions with an aberrant redox microenvironment, catalyzing endogenous substances to generate ROS for bacterial eradication.

### *Bone infections*

Bone tissue is a hard connective tissue with dynamic load-bearing functions and plays irreplaceable roles in the human body, including supporting and protecting soft tissues and organs, enabling movement, and hematopoiesis [144,145]. Post-traumatic bone infections are clinically common and have shown an increasing trend in recent years, particularly among the elderly and chronic patients. Such infections not only trigger inflammation and tissue destruction but also severely impede the bone healing process. Clinical treatments typically involve debridement and antibiotics, which carry risks of serious complications and antibiotic resistance [146,147]. Photothermal therapy, with its non-invasive nature and the ability to regulate the location and depth of irradiation, has garnered increasing attention as a treatment for bone infections [148,149]. Zhang *et al*. [150] synthesized $SiO_2$@ZnO core-shell nanoparticles via an ultrasound-assisted method and integrated them with poly(*L*-lactic acid) (PLLA) through electrospinning for photothermal and photodynamic antibacterial applications in bone repair (Figure 11c), followed by covalent attachment of poly-*L*-lysine (PLL) and PDA onto the fiber surface. Under NIR irradiation, PDA generated localized heat for antibacterial action, while ZnO nanoparticles penetrated bacterial cells and released $Zn^{2+}$ to inhibit intracellular enzyme activity and disrupt metabolism. PLL enhanced osteoblast adhesion and proliferation, thereby accelerating mineralization and bone regeneration. The resulting composite fibers exhibited rapid, light-responsive antibacterial activity and osteogenic potential, making them promising candidates for advanced bone repair.

### *Pulmonary infections*

Pneumonia is a common infectious disease and the sixth leading cause of death globally, as well as the primary cause of death in children under five [151]. Bacterial pneumonia [152] can cause symptoms such as cough and fever and may progress to fibrosis, chronic obstructive pulmonary disease, or death in severe cases [153]. The most common current treatment for bacterial pneumonia is antibiotics, which poses problems such as bacterial resistance and high recurrence rates. Therefore, there is an urgent need to develop novel, efficient treatments for bacterial pneumonia. *Klebsiella pneumoniae* (*K. pneumoniae*) is one of the common bacterial species causing bacterial pneumonia and is also associated with urinary tract and bloodstream infections [154]. Liu *et al*. [155] designed hollow mesoporous Prussian blue (HMPB) nanoparticles loaded with

ofloxacin and functionalized with hyaluronic acid (HA) (Figure 11d). The overexpression of HA enzymes on bacteria led to the release of ofloxacin from HMPB, combating the pathogen. Simultaneously, the photothermal effect of Prussian blue under light irradiation effectively killed bacteria. The synergy between ofloxacin and photothermal therapy reduced the required dose of ofloxacin and significantly enhanced the antibacterial effect against *K*. *pneumoniae*. The results indicate that Ofloxacin@HMPB@HA nanoparticles hold great potential for treating diseases caused by *K*. *pneumoniae* infections.

Tuberculosis (TB) is a severe infectious disease caused by *Mycobacterium tuberculosis* (*M*. *tuberculosis*), primarily affecting the lungs and posing a serious threat to global public health [156]. Li *et al*. [157] synthesized an aggregation-induced emission photothermal molecule (TPE-BT-BBTD) and encapsulated it in a poly(lactic-*co*-glycolic acid) (PLGA) core, followed by coating with macrophage cell membranes to form spherical core-shell nanoparticles. After intravenous administration in tuberculosis-infected mice, these nanoparticles rapidly accumulated in pulmonary granulomas and selectively targeted intracellular *M*. *tuberculosis* via receptor-ligand interactions. As Figure 12a shows, external 1064 nm laser irradiation induced photothermal conversion, achieving targeted bacterial killing while alleviating pulmonary tissue damage and inflammation. This strategy offers a potential therapeutic approach for both drug-sensitive and drug-resistant tuberculosis.

### *Other deep-seated infections*

Implant-associated infections typically occur in deep tissues, such as bone tissue, soft tissue interfaces, dental implant abutments, and around internal fixation materials. Ding *et al*. [158] loaded a thermosensitive CO donor, manganese pentacarbonyl bromide ($MnBr(CO)_5$), into PDA-modified $TiO_2$ hollow nanotubes to construct a photo-responsive CO nanocontainer (Figure 12b). Under NIR irradiation, photothermal effects from $TiO_2$ and PDA triggered $MnBr(CO)_5$ decomposition, enabling on-demand release of thermal CO bubbles. By integrating PTT with gas therapy, accelerated tissue regeneration at infected implant sites was achieved.

To provide a systematic overview of the currently reported hollow-structured photothermal synergistic antibacterial platforms, representative systems discussed in this review are summarized in Table 1 according to material category, hollow architecture, synergistic modality, and target infectious scenario.

## SUMMARY AND PERSPECTIVES

### Summary

This review systematically summarizes photothermal-synergistic therapeutic strategies based on hollow structures for diverse infection scenarios. First, the background of bacterial infections and the advantages of photothermal antibacterial therapy are outlined, highlighting the unique value of hollow structures in this field. Subsequently, the design and synthesis strategies of hollow-structured photothermal antibacterial materials are discussed from three perspectives: the principles of photothermal antibacterial therapy, photothermal performance enhancement mechanisms of hollow structures, and the design and synthesis of hollow-structured photothermal antibacterial systems. These discussions establish the material and theore-

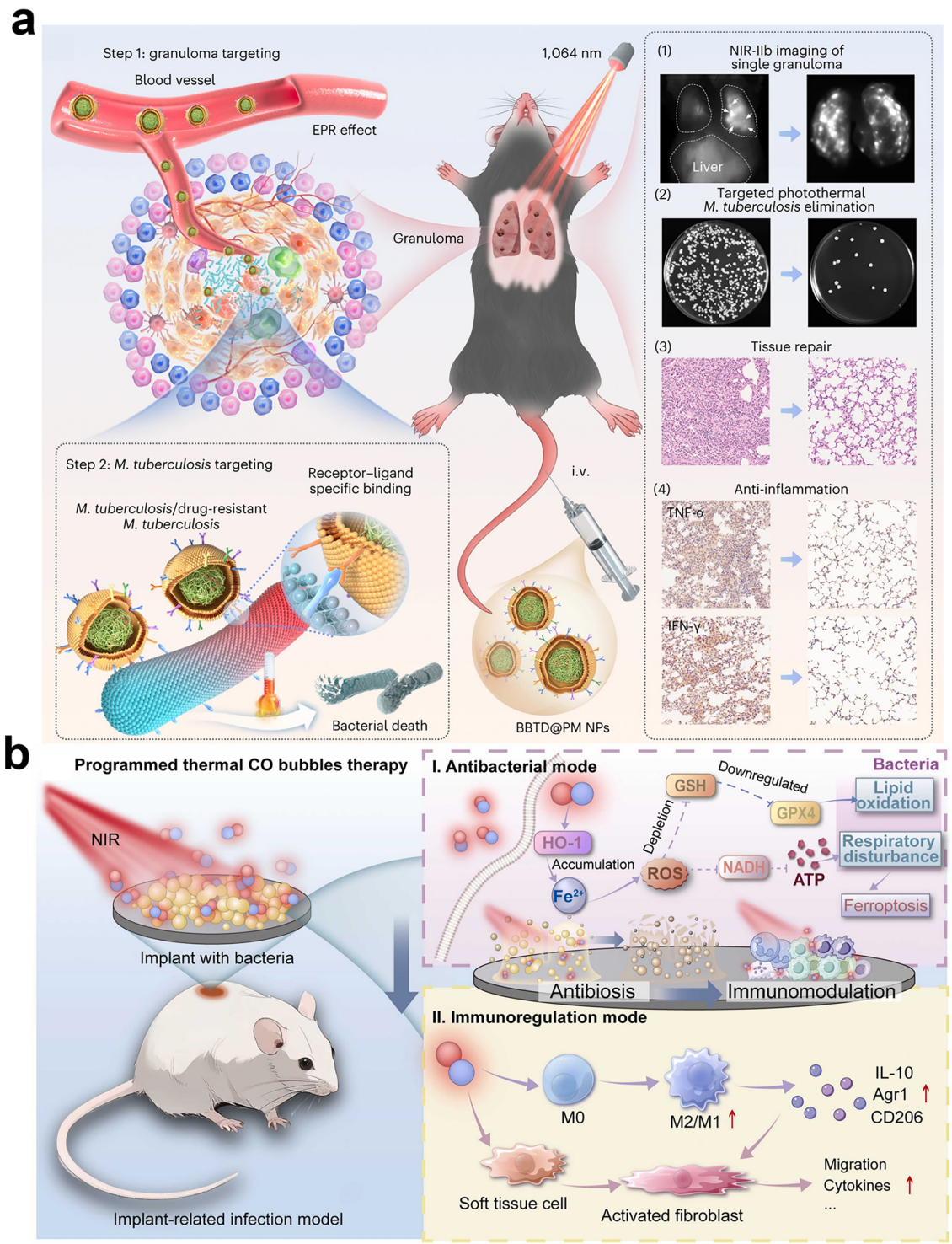


**Figure 12** (a) Schematic diagram for BBTD@PM NP-mediated lesion-pathogen dual targeting and NIR-IIb imaging-guided photothermal therapy for TB. EPR, enhanced permeability and retention; i.v., intravenous injection; TNF-α, tumour-necrosis factor-α; IFN-γ, interferon-γ. Reproduced with permission from Ref. [157]. Copyright©2024, The Author(s). (b) The programmed thermal CO bubbles therapy of COT for treating bacterial infection and modulating the inflammatory response to promote fibroblast response and tissue repair. Reproduced with permission from Ref. [158]. Copyright©2025, Elsevier Ltd.

tical foundations for multifunctional photothermal-synergistic antibacterial platforms.

The inherent limitations of photothermal monotherapy are then addressed, followed by a comprehensive overview of photothermal-synergistic antibacterial strategies enabled by hollow structures, including PDT, CDT, drug therapy, and gas therapy, together with their synergistic enhancement mechanisms. Finally, by reviewing the application progress of these platforms in different clinical settings, ranging from superficial wound infections to deep-seated infections, the feasibility and significant potential of hollow structures for photothermal synergistic treatment of multiple infection scenarios are fully demonstrated.

## Challenges and perspectives

Although hollow-structured photothermal nanoplatforms demonstrate significant advantages and have achieved extensive progress in antibacterial therapy, their translation into practical applications and clinical use still faces challenges. These challenges encompass not only the biosafety of the materials, but also the feasibility of large-scale fabrication and quality control, as well as technical bottlenecks in achieving safe, precise, and controllable photothermal therapy in complex clinical scenarios. Systematically addressing and confronting these issues is of great importance for promoting the development of hollow-structured photothermal antibacterial nanoplatforms from laboratory to practical applications.

### *Challenges*

Biological safety of hollow structures remains a critical concern. Hollow structures, including inorganic materials (such as metal sulfides and noble metals), inorganic-organic hybrid materials and organic nanomaterials, often lack systematic investigations into their long-term biocompatibility, degradation products, and metabolic pathways, which may pose potential risks to human health.

Large-scale fabrication of hollow structures faces substantial challenges. At present, the synthesis of hollow structures is largely confined to laboratory-scale studies, with relatively high production costs and complex procedures, hindering scalable, cost-effective, and efficient manufacturing. Owing to their nanoscale nature, achieving high product uniformity remains challenging, and batch-to-batch variability can result in inconsistent performance. In addition, the development of stable formulations that are suitable for storage, transportation, and practical application in photothermal antibacterial therapy remains challenging.

Limited NIR light penetration restricts photothermal therapy application for deep-tissue infections. Moreover, during photothermal conversion, hollow PTAs may cause thermal damage or chemical toxicity to healthy tissues while eradicating pathogens, necessitating precise control over irradiation sites and real-time temperature monitoring. Although synergistic photothermal strategies are widely explored, many studies emphasize therapeutic outcomes while providing insufficient mechanistic insight into the interplay between PTT and complementary modalities.

### *Perspectives*

(1) Intelligent design of biodegradable hollow structures. Bacterial biofilms, characterized by dense EPS matrices, negatively charged surfaces, and infection-specific microenvironments, significantly hinder drug

**Table 1** Summary of hollow-structured photothermal synergistic antibacterial platforms

| Material category | Composition | Hollow structure type | Synergistic modality | Target infection scenario | Ref. |
|---|---|---|---|---|---|
| Metal-based | Ag-Au nanoparticles | Single-shelled | PTT+PDT | Wound infection | [95] |
| | Bi nanospheres | Single-shelled | PTT+gas therapy (CO) | Infected wound healing. | [105] |
| | Au nanocage | Single-shelled | PTT+gas therapy (NO) | Biofilm-associated infections | [109] |
| | Au-Ag nanoparticles | Core-Shell | PTT+Ag ion release | Superficial wound infection | [121] |
| | Au-Ag nanoparticles | Single-shelled | PTT+drug therapy | Endophthalmitis | [138] |
| | Au nanocages | Single-shelled | PTT+drug therapy | Periodontitis | [140] |
| Metal sulfide/metal oxide-based | $MnO_x$ nanozyme | Single-shelled | PTT+CDT | Bacterial infections | [25] |
| | CuO nanoparticles | Single-shelled | PTT+CDT | Bacterial infections | [26] |
| | $Bi_2S_3$ microspheres | Single-shelled | PTT+drug therapy | Bacterial infections | [96] |
| | $Au@Bi_2S_3$ nanostructures | Core-Shell | PTT+PDT | Bacterial infections | [98] |
| | Mo single-atom nanozymes | Single-shelled | PTT+CDT | Diabetic wound healing | [126] |
| | $FeCoO_x$ nanoparticles | Multi-shelled | PTT+PDT | Bacterial keratitis | [133] |
| | $SiO_2@ZnO$ nanoparticles | Core-Shell | PTT+PDT | Bone infection | [150] |
| Organic polymers-based | PDA microspheres | Single-shelled | PTT+drug therapy | Bacterial infections | [97] |
| | PDA-coated ZnO | Core-Shell | PTT+PDT | Superficial wound | [122] |
| | PDA-modified $TiO_2$ nanotubes | Single-shelled | PTT+gas therapy (CO) | Implant-associated infection | [158] |

diffusion and reduce the efficacy of PTT. The rational design of biodegradable hollow-structured photothermal nanoplatforms plays a critical role in advancing antibacterial therapy, particularly for overcoming the key challenge of biofilm penetration and eradication. Therefore, the rational design of hollow-structured photothermal nanoplatforms should integrate biocompatibility, structural controllability, and biofilm-targeting or microenvironment-responsive functionalities to improve antibacterial efficacy in complex infectious conditions.

At the material and structural levels, biocompatibility and metabolic controllability remain fundamental requirements. Priority should be given to using building blocks that have been proven to have good biocompatibility or metabolizable components. For example, biodegradable PTAs like PDA [159] are promising due to their simple preparation and good biocompatibility. Their abundant amino and catechol groups also allow for reactions with other components [160] or modification with specific functional groups [161]. Copper sulfides not only exhibit excellent photothermal properties, but their degradation products, copper ions, also possess antibacterial functions and may enhance therapeutic efficacy through new mechanisms called cuproptosis [162]. Meanwhile, rational hollow-structure engineering, such as shell modulation or the construction of HoMS, can improve local heat confinement and provide sufficient internal space for the loading and controlled release of therapeutic agents, thereby enhancing the disruption of the EPS matrix and supporting biofilm eradication. However, the long-term metabolic fate and accumulation-related toxicity of these materials *in vivo* still need further clarification.

More importantly, microenvironment-responsive design provides an effective strategy for improving biofilm penetration. Infection sites are typically characterized by acidic pH, elevated $H_2O_2$ levels, and enzyme overexpression, which can be exploited to trigger structural transformation, charge reversal, or controlled drug release. For instance, in acidic or $H_2O_2$-rich microenvironments, hollow manganese oxides can undergo pH-responsive decomposition to release $Mn^{2+}$ and loaded drugs, or directly react with overexpressed $H_2O_2$ to consume the harmful peroxide and generate oxygen *in situ*, alleviating tissue hypoxia.

Alternatively, specific functional groups like pyridinium betaine [163] or thioacetamide [164] can be grafted onto the hollow structure surface to induce charge reversal in acidic environments, enhancing biofilm penetration. To respond to enzymes over-secreted by bacteria, peptides or polysaccharides degradable by these specific enzymes can be used as gatekeepers on the hollow structure surface, achieving localized, intelligent, responsive drug release at bacterial aggregation sites.

Finally, for complex pathological conditions (e.g., diabetic infected wounds), integrating functions such as cascaded catalytic activities to construct "all-in-one" therapeutic platforms. For example, photothermal hollow structures can be loaded with glucose oxidase to decompose glucose, generate $H_2O_2$, and lower pH. They can also possess catalase-like activity to decompose $H_2O_2$ into oxygen, reducing oxidative stress levels and alleviating wound hypoxia. This cascade-reaction strategy [165,166] targeting diabetic wounds facilitates multi-mechanism synergy, promoting wound healing alongside photothermal antibacterial action. These multifunctional platforms represent an important direction for the future development of intelligent antibacterial nanomaterials.

(2) Exploring scalable fabrication methods for hollow structures. Current preparation methods for hollow structures include the hard-template method, soft-template method and self-template method. Both hard- and soft-template methods involve template selection and removal. Although these techniques are relatively mature and allow precise control over morphology and size, they are often multi-step and time-consuming. In contrast, the self-template method generates hollow structures through physicochemical processes like particle diffusion or self-assembly without external templates, offering advantages such as lower cost, simplicity, high reproducibility, and good control over shell thickness and particle uniformity. Therefore, the self-template method should be prioritized for future synthesis of hollow structures to achieve scalable production. The mechanisms of the self-template method primarily fall into three categories: selective etching, outward diffusion, and non-uniform contraction [167]. Understanding these mechanisms will facilitate researchers in utilizing the self-template method for scalable fabrication, and combining these mechanisms can enable the synthesis of complex hollow structures [168].

Furthermore, integrating conventional hollow structure preparation methods with synthesis concepts from other nanomaterials can improve hollow structure synthesis. For example, Yang *et al*. [169] proposed a novel concept combining template methods with polymer gel soft matter to induce the localized growth of functional materials. Leveraging the permeability of gels and their ease of compounding with functional substances, they developed a new scalable method for preparing hollow microspheres with tunable shell thickness and cavity size.

(3) Development of novel PTAs and synergistic therapeutic strategies. To overcome the limited penetration depth of near-infrared light, future efforts should focus on developing new-generation PTAs and therapeutic strategies. In terms of materials, active advancement should be made toward NIR-II-responsive materials or the construction of multi-physical field synergistic excitation systems, such as photo-acoustic/magnetic-thermal combinations, to enhance energy penetration and treatment depth, thereby expanding their application potential in deep tissue infections. In therapeutic strategies, it is essential to investigate deeply the interaction mechanisms and synergistic principles between PTT and other treatments (e.g., CDT, PDT, gas therapy). For instance, research could investigate how the localized thermal effects generated by PTT enhance the ROS produced in PDT, thereby promoting bacterial clearance, or how PTT synergizes with gas therapy. Understanding these synergistic mechanisms is crucial for designing novel and efficient synergistic

strategies, achieving higher therapeutic efficacy, and reducing the risk of side effects.

By exploring these directions, it is expected that the bottlenecks of hollow-structured photothermal antibacterial platforms, such as biosafety, treatment depth, and synergistic efficacy, can be systematically addressed, accelerating their clinical translation process.

## Funding

This work was supported by the Beijing Natural Science Foundation (2262078), the Shenzhen University 2035 Program for Excellent Research (2024B005), the Open Funding Project of the State Key Laboratory of Biopharmaceutical Preparation and Delivery (2023KF-04), the National Natural Science Foundation of China (22293043), and the National Key Research and Development Program of China (2024YFA1509400). D.W. thanks the financial support from the Outstanding Scientific and Technological Innovation Talents Training Fund in Shenzhen.

## Author contributions

N.K. conducted literature collection, wrote the original draft and revised the manuscript. D.Z. provided topic selection, framework design and manuscript review. J.W. participated in discussion and manuscript revision. D.W. provided academic guidance of the entire manuscript. All authors read and approved the final manuscript.

## Conflict of interest

The authors declare no conflict of interest.

## References

1 Brown ED, Wright GD. Antibacterial drug discovery in the resistance era. *Nature* 2016; **529**: 336–343.

2 Richter MF, Drown BS, Riley AP, *et al.* Predictive compound accumulation rules yield a broad-spectrum antibiotic. *Nature* 2017; **545**: 299–304.

3 Savage VJ, Chopra I, O'Neill AJ. *Staphylococcus aureus* biofilms promote horizontal transfer of antibiotic resistance. *Antimicrob Agents Chemother* 2013; **57**: 1968–1970.

4 Flemming HC, Wuertz S. Bacteria and archaea on Earth and their abundance in biofilms. *Nat Rev Microbiol* 2019; **17**: 247–260.

5 Ciofu O, Tolker-Nielsen T. Tolerance and resistance of *Pseudomonas aeruginosa* biofilms to antimicrobial agents—How *P. aeruginosa* can escape antibiotics. *Front Microbiol* 2019; **10**: 913.

6 Rather MA, Gupta K, Mandal M. Microbial biofilm: Formation, architecture, antibiotic resistance, and control strategies. *Braz J Microbiol* 2021; **52**: 1701–1718.

7 Katre DD, Deb M. A review on biofilms. *J Pharm Res Int* 2021; **33**: 1021–1026.

8 Tamma PD, Avdic E, Li DX, *et al.* Association of adverse events with antibiotic use in hospitalized patients. *JAMA Intern Med* 2017; **177**: 1308–1315.

9 Hagiya H, Kokado R, Ueda A, *et al.* Association of adverse drug events with broad-spectrum antibiotic use in hospitalized patients: A single-center study. *Intern Med* 2019; **58**: 2621–2625.

10 Levy SB, Marshall B. Antibacterial resistance worldwide: Causes, challenges and responses. *Nat Med* 2004; **10**: S122–S129.

11 Advocating for phage therapy. *Nat Microbiol* 2024; **9**: 1397–1398 .

12 Sunderland KS, Yang M, Mao C. Phage-enabled nanomedicine: From probes to therapeutics in precision medicine. *Angew Chem Int Ed* 2017; **56**: 1964–1992.

13 Gao S, Yan X, Xie G, *et al.* Membrane intercalation-enhanced photodynamic inactivation of bacteria by a metallacycle and TAT-decorated virus coat protein. *Proc Natl Acad Sci USA* 2019; **116**: 23437–23443.

14 Gnanasekar S, Kasi G, He X, *et al.* Recent advances in engineered polymeric materials for efficient photodynamic inactivation of bacterial pathogens. *Bioactive Mater* 2023; **21**: 157–174.

15 He P, Jia M, Yang L, *et al.* Zwitterionic photosensitizer-assembled nanocluster produces efficient photogenerated radicals via autoionization for superior antibacterial photodynamic therapy. *Adv Mater* 2025; **37**: e2418978.

16 Wang Y, Zhao L, Li Z, *et al.* A generative artificial intelligence approach for the discovery of antimicrobial peptides against multidrug-resistant bacteria. *Nat Microbiol* 2025; **10**: 2997–3012.

17 Dijksteel GS, Ulrich MMW, Middelkoop E, *et al.* Lessons learned from clinical trials using antimicrobial peptides. *Front Microbiol* 2021; **12**: 616979.

18 Guan G, Win KY, Yao X, *et al.* Plasmonically modulated gold nanostructures for photothermal ablation of bacteria. *Adv Healthc Mater* 2021; **10**: 2001158.

19 Li X, Lovell JF, Yoon J, *et al.* Clinical development and potential of photothermal and photodynamic therapies for cancer. *Nat Rev Clin Oncol* 2020; **17**: 657–674.

20 Yi J, Liu L, Gao W, *et al.* Advances and perspectives in phototherapy-based combination therapy for cancer treatment. *J Mater Chem B* 2024; **12**: 6285–6304.

21 Yang S, Liu J, Yuan H, *et al.* Synergistic photothermal therapy and chemotherapy enabled by tumor microenvironment-responsive targeted swcnt delivery. *Int J Mol Sci* 2024; **25**: 9177.

22 Xie M, Gao M, Yun Y, *et al.* Antibacterial nanomaterials: Mechanisms, impacts on antimicrobial resistance and design principles. *Angew Chem Int Ed* 2023; **62**: e202217345.

23 Zhao D, Yang N, Wei Y, *et al.* Sequential drug release via chemical diffusion and physical barriers enabled by hollow multishelled structures. *Nat Commun* 2020; **11**: 4450.

24 Sheng C, Ding Y, Guo M. Compartmentalization into outer and inner shells of hollow nanospheres for antibiosis based on chemistry and physical damages. *Adv Healthc Mater* 2024; **13**: e2400851.

25 Wu H, Wei M, Hu S, *et al.* A photomodulable bacteriophage-spike nanozyme enables dually enhanced biofilm penetration and bacterial capture for photothermal-boosted catalytic therapy of mrsa infections. *Adv Sci* 2023; **10**: e2301694.

26 Shi H, Ban C, Dai C, *et al.* Glutathione-depletion reinforced enzyme catalytic activity for photothermal assisted bacterial killing by hollow mesoporous CuO. *J Mater Chem B* 2022; **10**: 8883–8893.

27 Zhao D, Wei Y, Jin Q, *et al.* PEG-functionalized hollow multishelled structures with on-off switch and rate-regulation for controllable antimicrobial release. *Angew Chem Int Ed* 2022; **61**: e202206807.

28 Sun X, He G, Xiong C, *et al.* One-pot fabrication of hollow porphyrinic mof nanoparticles with ultrahigh drug loading toward controlled delivery and synergistic cancer therapy. *ACS Appl Mater Interfaces* 2021; **13**: 3679–3693.

29 Song C, Wang Z, Yin Z, *et al.* Principles and applications of photothermal catalysis. *Chem Catal* 2022; **2**: 52–83.

30 Xu D, Li Z, Li L, *et al.* Insights into the photothermal conversion of 2D MXene nanomaterials: synthesis, mechanism, and applications. *Adv Funct Mater* 2020; **30**: 2070314.

31 Li L, Zhang X, Zhou J, *et al.* Non-invasive thermal therapy for tissue engineering and regenerative medicine. *Small* 2022; **18**: e2107705.

32 Asahi R, Morikawa T, Ohwaki T, *et al.* Visible-light photocatalysis in nitrogen-doped titanium oxides. *Science* 2001; **293**: 269–271.

33 Prieto G, Tüysüz H, Duyckaerts N, *et al.* Hollow nano- and microstructures as catalysts. *Chem Rev* 2016; **116**: 14056–14119.

34 Dong Z, Lai X, Halpert JE, *et al.* Accurate control of multishelled zno hollow microspheres for dye-sensitized solar cells with high efficiency. *Adv Mater* 2012; **24**: 1046–1049.

35 Lien D, Dong Z, Retamal JRD, *et al.* Resonance-enhanced absorption in hollow nanoshell spheres with omnidirectional detection and high responsivity and speed. *Adv Mater* 2018; **30**: 1801972.

36 Chen J, Feng J, Yang F, *et al.* Space-confined seeded growth of Cu nanorods with strong surface plasmon resonance for photothermal actuation. *Angew Chem Int Ed* 2019; **58**: 9275–9281.

37 Brongersma ML, Halas NJ, Nordlander P. Plasmon-induced hot carrier science and technology. *Nat Nanotech* 2015; **10**: 25–34.

38 Chen H, Shao L, Ming T, *et al.* Understanding the photothermal conversion efficiency of gold nanocrystals. *Small* 2010; **6**: 2272–2280.

39 Jain PK, Huang X, El-Sayed IH, *et al.* Noble metals on the nanoscale: Optical and photothermal properties and some applications in imaging, sensing, biology, and medicine. *Acc Chem Res* 2008; **41**: 1578–1586.

40 Kale MJ, Avanesian T, Christopher P. Direct photocatalysis by plasmonic nanostructures. *ACS Catal* 2014; **4**: 116–128.

41 Shao S, Xia X. Engineering the internal structure of hollow nanostructures for enhanced plasmonic properties. *J Phys Chem C* 2024; **128**: 10761–10773.

42 Wang P, Huang B, Lou Z, *et al.* Synthesis of highly efficient Ag@AgCl plasmonic photocatalysts with various structures. *Chem Eur J* 2010; **16**: 538–544.

43 Wei Y, Wang Z, Yu R. Highly efficient photothermal conversion media: Hollow multishelled structural materials. Chin Sci Bull 2019; **64**: 3577–3593 .

44 Thaweesak S, Lyu M, Peerakiatkhajohn P, *et al.* Two-dimensional g-$C_3N_4$/$Ca_2Nb_2TaO_{10}$ nanosheet composites for efficient visible light photocatalytic hydrogen evolution. *Appl Catal B-Environ* 2017; **202**: 184–190.

45 He X, Wu H, Xu K, *et al.* Biomimetic engineering of robust gradient antibacterial coatings using hollow nanoframes of prussian blue analogues. *Adv Mater* 2025; **37**: e2501174.

46 Yu Y, Tian R, Zhao Y, *et al.* Self-assembled corrole/chitosan photothermal nanoparticles for accelerating infected diabetic wound healing. *Adv Healthc Mater* 2023; **12**: 2201651.

47 Xiong Q, Fang Q, Xu K, *et al.* Near-infrared light-responsive photothermal α-$Fe_2O_3$@Au/PDA core/shell nanostructure with on–off controllable anti-bacterial effects. *Dalton Trans* 2021; **50**: 14235–14243.

48 Mao D, Wang C, Li W, *et al.* Hollow multishelled structure: Synthesis chemistry and application. *Chem Res Chin Univ* 2024; **40**: 346–393.

49 Hou P, Yang N, Wang D. Multi-functional hollow structures for intelligent drug delivery. *Chem Res Chin Univ* 2024; **40**: 394–412.

50 Chen X, Yang N, Wang Y, *et al.* Highly efficient photothermal conversion and water transport during solar evaporation enabled by amorphous hollow multishelled nanocomposites. *Adv Mater* 2022; **34**: e2107400.

51 Shi X, Yu Y, Yu R, *et al.* Facile synthesis of copper sulfide loaded mesoporous organosilica nanospheres with a triple-shelled hollow structure. *J Porous Mater* 2025; **32**: 67–74.

52 Lee J, Hwang S, Yun J, *et al.* Fabrication of $SiO_2$/$TiO_2$ double-shelled hollow nanospheres with controllable size via sol-gel reaction and sonication-mediated etching. *ACS Appl Mater Interfaces* 2014; **6**: 15420–15426.

53 Liu H, Ma Z, Zhang C, *et al.* Optical properties of hollow plasmonic nanopillars for efficient solar photothermal conversion. *Renew Energy* 2023; **208**: 251–262.

54 Qi X, Huang Y, You S, *et al.* Engineering robust Ag-decorated polydopamine nano-photothermal platforms to combat bacterial infection and prompt wound healing. *Adv Sci* 2022; **9**: e2106015.

55 Qiao Y, Ping Y, Zhang H, *et al.* Laser-activatable cus nanodots to treat multidrug-resistant bacteria and release copper ion to accelerate healing of infected chronic nonhealing wounds. *ACS Appl Mater Interfaces* 2019; **11**: 3809–3822.

56 Chou SS, Kaehr B, Kim J, *et al.* Chemically exfoliated $MoS_2$ as near-infrared photothermal agents. *Angew Chem Int Ed* 2013; **52**: 4160–4164.

57 Bai Y, Zhao J, Zhang L, *et al.* A smart near-infrared carbon dot-metal organic framework assemblies for tumor microenvironment-activated cancer imaging and chemodynamic-photothermal combined therapy. *Adv Healthc Mater* 2022; **11**: e2102759.

58 Tian B, Liu S, Feng L, *et al.* Renal-clearable nickel-doped carbon dots with boosted photothermal conversion efficiency for multimodal imaging-guided cancer therapy in the second near-infrared biowindow. *Adv Funct Mater* 2021; **31**: 2100549.

59 Gong F, Wang W, Li H, *et al.* Solid waste and graphite derived solar steam generator for highly-efficient and cost-

effective water purification. *Appl Energy* 2020; **261**: 114410.

60 Li T, Liu H, Zhao X, *et al.* Scalable and highly efficient mesoporous wood-based solar steam generation device: Localized heat, rapid water transport. *Adv Funct Mater* 2018; **28**: 1707134.

61 Zhao Y, Zhao T, Cao Y, *et al.* Temperature-sensitive lipid-coated carbon nanotubes for synergistic photothermal therapy and gene therapy. *ACS Nano* 2021; **15**: 6517–6529.

62 Chen C, Li Y, Song J, *et al.* Highly flexible and efficient solar steam generation device. *Adv Mater* 2017; **29**: 1701756.

63 Xie Y, Li W, Huang H, *et al.* Bio-based radish@PDA/PEG sandwich composite with high efficiency solar thermal energy storage. *ACS Sustain Chem Eng* 2020; **8**: 8448–8457.

64 Yoon HJ, Lee HS, Lim JY, *et al.* Liposomal indocyanine green for enhanced photothermal therapy. *ACS Appl Mater Interfaces* 2017; **9**: 5683–5691.

65 Yu Y, Song M, Chen C, *et al.* Bortezomib-encapsulated cus/carbon dot nanocomposites for enhanced photothermal therapy via stabilization of polyubiquitinated substrates in the proteasomal degradation pathway. *ACS Nano* 2020; **14**: 10688–10703.

66 Deng X, Li K, Cai X, *et al.* A hollow-structured CuS@$Cu_2S$@Au nanohybrid: Synergistically enhanced photothermal efficiency and photoswitchable targeting effect for cancer theranostics. *Adv Mater* 2017; **29**: 1701266.

67 Wang H, Shen Y, Chen L, *et al.* Enhancing catalase-like activity of Prussian blue nanozyme by gadolinium-doping for imaging-guided antitumor amplification via photodynamic therapy and chemotherapy. *Mater Today Nano* 2023; **22**: 100326.

68 Chen Z, Zhang L, Yang Y, *et al.* Photothermal nanozyme-encapsulating microneedles for synergistic treatment of infected wounds. *Adv Funct Mater* 2025; **35**: 2417415.

69 Zhang M, Hu X, Huang Y. Hollow semimetal PtTe nanorods with high performance for photothermal/photodynamic/chemodynamic therapy in the NIR-II window. *Colloids Surfs B-Biointerfaces* 2025; **254**: 114835.

70 Xu Q, Li J, Liu B, *et al.* Biodegradable copper-doped hollow mesoporous polydopamine nanoparticles for chemo/photothermal/chemodynamic synergistic therapy. *J Drug Deliver Sci Tech* 2023; **89**: 105015.

71 Kong J, Ma S, Chu R, *et al.* Photothermal and photocatalytic glycol chitosan and polydopamine-grafted oxygen vacancy bismuth oxyiodide ($BiO_{1-x}I$) nanoparticles for the diagnosis and targeted therapy of diabetic wounds. *Adv Mater* 2024; **36**: e2307695.

72 Ye Y, Zeng X, Luo Z, *et al.* Enhanced photostability and targeting ability of hollow mesoporous manganese-based nanocarriers for NIR-II fluorescence image-guided surgery and photothermal therapy. *J Colloid Interface Sci* 2025; **698**: 138094.

73 Wang X, Song Q, Sun B, *et al.* Bacteria-targeting nanozyme with NIR-II photothermal enhanced catalytic effect for antibacterial therapy and promoting burn healing. *Colloids Surfs A-Physicochem Eng Aspects* 2023; **674**: 131902.

74 Zhang Y, Wang D, Liu F, *et al.* Enhancing the drug sensitivity of antibiotics on drug-resistant bacteria via the photothermal effect of FeTGNPs. *J Control Release* 2022; **341**: 51–59.

75 Xing Z, Dong B, Zhang X, *et al.* Cypate-loaded hollow mesoporous Prussian blue nanoparticle/hydrogel system for efficient photodynamic therapy/photothermal therapy dual-modal antibacterial therapy. *J BioMed Mater Res* 2024; **112**: 53–64.

76 Bao Y, Yang YQ, Ma JZ. Research progress of hollow structural materials prepared via templating method. *J InOrg Mater* 2013; **28**: 459–468.

77 Zhang G, Wu HB, Song T, *et al.* $TiO_2$ hollow spheres composed of highly crystalline nanocrystals exhibit superior lithium storage properties. *Angew Chem Int Ed* 2014; **53**: 12590–12593.

78 Hwang SH, Yun J, Jang J. Multi-shell porous $TiO_2$ hollow nanoparticles for enhanced light harvesting in dye-sensitized solar cells. *Adv Funct Mater* 2014; **24**: 7619–7626.

79 Lai X, Li J, Korgel BA, *et al.* General synthesis and gas-sensing properties of multiple-shell metal oxide hollow microspheres. *Angew Chem Int Ed* 2011; **50**: 2738–2741.

80 Mao D, Wan J, Wang J, *et al.* Sequential templating approach: A groundbreaking strategy to create hollow multishelled

structures. *Adv Mater* 2019; **31**: 1802874.

81 Wei Y, You F, Zhao D, *et al.* Heterogeneous hollow multi-shelled structures with amorphous-crystalline outer-shells for sequential photoreduction of $CO_2$. *Angew Chem Int Ed* 2022; **61**: e202212049.

82 Zhang H, Zhang S, Guo B, *et al.* $MoS_2$ hollow multishelled nanospheres doped Fe single atoms capable of fast phase transformation for fast-charging Na-ion batteries. *Angew Chem Int Ed* 2024; **63**: e202400285.

83 Mason TG, Wilking JN, Meleson K, *et al.* Nanoemulsions: Formation, structure, and physical properties. *J Phys-Condens Matter* 2006; **18**: R635–R666.

84 Xu H, Wang W. Template synthesis of multishelled $Cu_2O$ hollow spheres with a single-crystalline shell wall. *Angew Chem Int Ed* 2007; **46**: 1489–1492.

85 Fujii Y, Zhou S, Shimada M, *et al.* Synthesis of monodispersed hollow mesoporous organosilica and silica nanoparticles with controllable shell thickness using soft and hard templates. *Langmuir* 2023; **39**: 4571–4582.

86 Liang Y, Yu Y, Qi X. Synthesis of hollow hierarchical porous carbon spheres from lignin by soft template and hydrothermal method for supercapacitors. *Int J Biol Macromol* 2025; **307**: 141938.

87 Feng J, Yin Y. Self-templating approaches to hollow nanostructures. *Adv Mater* 2019; **31**: e1802349.

88 Xiong S, Zeng HC. Serial ionic exchange for the synthesis of multishelled copper sulfide hollow spheres. *Angew Chem Int Ed* 2012; **51**: 949–952.

89 Zhang T, Ge J, Hu Y, *et al.* Formation of hollow silica colloids through a spontaneous dissolution-regrowth process. *Angew Chem Int Ed* 2008; **47**: 5806–5811.

90 Wang Z, Wang Z, Wu H, *et al.* Mesoporous single-crystal $CoSn(OH)_6$ hollow structures with multilevel interiors. *Sci Rep* 2013; **3**: 1391.

91 Zhang C, Bu W, Ni D, *et al.* Synthesis of iron nanometallic glasses and their application in cancer therapy by a localized fenton reaction. *Angew Chem Int Ed* 2016; **55**: 2101–2106.

92 Xu X, Zeng Z, Chen J, *et al.* Tumor-targeted supramolecular catalytic nanoreactor for synergistic chemo/chemodynamic therapy via oxidative stress amplification and cascaded Fenton reaction. *Chem Eng J* 2020; **390**: 124628.

93 Liu JH, She QM, Li CJ, *et al.* Thermosensitive hydrogel loaded with the polydopamine/cerium dioxide/montmorillonite nanocomposite for bacteria-infected wound therapy. *ACS Appl Nano Mater* 2024; **7**: 24522–24536.

94 Obaid G, Celli JP, Broekgaarden M, *et al.* Engineering photodynamics for treatment, priming and imaging. *Nat Rev Bioeng* 2024; **2**: 752–769.

95 Lin S, Chen H, Wang R, *et al.* Hollow silver–gold alloy nanoparticles for enhanced photothermal/photodynamic synergetic therapy against bacterial infection and acceleration of wound healing. *BioMater Sci* 2023; **11**: 4874–4889.

96 Wang WN, Zhang CY, Zhang MF, *et al.* Precisely photothermal controlled releasing of antibacterial agent from $Bi_2S_3$ hollow microspheres triggered by NIR light for water sterilization. *Chem Eng J* 2020; **381**: 122630.

97 Gao L, Lu W, Chen Y, *et al*. Preparation and anti-infection research of ciprofloxacin-loaded polydopamine hollow microspheres. Chin J Mod Appl Pharm 2023; **40**: 2268–2276 .

98 Wang WN, Pei P, Chu ZY, *et al.* $Bi_2S_3$ coated Au nanorods for enhanced photodynamic and photothermal antibacterial activities under NIR light. *Chem Eng J* 2020; **397**: 125488.

99 Yan Z, Liu Z, Zhang H, *et al.* Current trends in gas-synergized phototherapy for improved antitumor theranostics. *Acta Biomater* 2024; **174**: 1–25.

100 Xu M, Wu G, You Q, *et al.* The landscape of smart biomaterial-based hydrogen therapy. *Adv Sci* 2024; **11**: e2401310.

101 Chen M, Xu T, Song L, *et al.* Nanotechnology based gas delivery system: A “green” strategy for cancer diagnosis and treatment. *Theranostics* 2024; **14**: 5461–5491.

102 Hu H, Li D, Dai W, *et al.* A NIR-II AIEgen-based supramolecular nanodot for peroxynitrite-potentiated mild-temperature photothermal therapy of hepatocellular carcinoma. *Adv Funct Mater* 2023; **33**: 2213134.

103 You C, Li Y, Dong Y, *et al.* Low-temperature trigger nitric oxide nanogenerators for enhanced mild photothermal therapy. *ACS BioMater Sci Eng* 2020; **6**: 1535–1542.

104 García-Gallego S, Bernardes GJL. Carbon-monoxide-releasing molecules for the delivery of therapeutic CO *in vivo*. *Angew Chem Int Ed* 2014; **53**: 9712–9721.

105 Lv D, Xu Z, Yang H, *et al.* Hollow bismuth nanoparticle-loaded gelatin hydrogel regulates M2 polarization of macrophages to promote infected wound healing. *BioMater Res* 2024; **28**: 0105.

106 Malone-Povolny MJ, Maloney SE, Schoenfisch MH. Nitric oxide therapy for diabetic wound healing. *Adv Healthc Mater* 2019; **8**: e1801210.

107 Wang J, Wang L, Pan J, *et al.* Magneto-based synergetic therapy for implant-associated infections via biofilm disruption and innate immunity regulation. *Adv Sci* 2021; **8**: 2004010.

108 Rouillard K, Novak O, Pistiolis A, *et al.* Exogenous nitric oxide improves antibiotic susceptibility in resistant bacteria. *ACS Infect Dis* 2021; **7**: 23–33.

109 Tang Y, Wang T, Feng J, *et al.* Photoactivatable nitric oxide-releasing gold nanocages for enhanced hyperthermia treatment of biofilm-associated infections. *ACS Appl Mater Interfaces* 2021; **13**: 50668–50681.

110 Qi M, Ren X, Li W, *et al.* NIR responsive nitric oxide nanogenerator for enhanced biofilm eradication and inflammation immunotherapy against periodontal diseases. *Nano Today* 2022; **43**: 101447.

111 Cao J, Qiu S, Wang M, *et al.* Smart response CO hydrogel "battling" bacterial biofilms and inflammation associated with wounds. *J Hazard Mater* 2025; **490**: 137662.

112 Son S, Kim JH, Wang X, *et al.* Multifunctional sonosensitizers in sonodynamic cancer therapy. *Chem Soc Rev* 2020; **49**: 3244–3261.

113 Li Y, Chen W, Kang Y, *et al.* Nanosensitizer-mediated augmentation of sonodynamic therapy efficacy and antitumor immunity. *Nat Commun* 2023; **14**: 6973.

114 Feigal EG, DeWitt ND, Cantilena C, *et al.* At the end of the beginning: Immunotherapies as living drugs. *Nat Immunol* 2019; **20**: 955–962.

115 Yuan X, Zhou JL, Yuan L, *et al.* Phototherapy: Progress, challenges, and opportunities. *Sci China Chem* 2025; **68**: 826–865.

116 Bai X, Yang Y, Zheng W, *et al.* Synergistic photothermal antibacterial therapy enabled by multifunctional nanomaterials: Progress and perspectives. *Mater Chem Front* 2023; **7**: 355–380.

117 Zhao Y, Zhao Y, Xu B, *et al.* Microenvironmental dynamics of diabetic wounds and insights for hydrogel-based therapeutics. *J Tissue Eng* 2024; **15**: 20417314241253290.

118 Ramos MDN, Lima JPP, Aguiar A. Determination of activation energy from decolorization reactions of synthetic dyes by fenton processes using the behnajady–modirshahla–ghanbary kinetic model. *Catalysts* 2024; **14**: 273.

119 Tang S, Zheng J. Antibacterial activity of silver nanoparticles: Structural effects. *Adv Healthc Mater* 2018; **7**: 1701503.

120 Rizzello L, Pompa PP. Nanosilver-based antibacterial drugs and devices: Mechanisms, methodological drawbacks, and guidelines. *Chem Soc Rev* 2014; **43**: 1501–1518.

121 He J, Qiao Y, Zhang H, *et al.* Gold–silver nanoshells promote wound healing from drug-resistant bacteria infection and enable monitoring via surface-enhanced Raman scattering imaging. *Biomaterials* 2020; **234**: 119763.

122 Salehi N, Mohammadi A, Alinezhad V, *et al.* Synergistic photothermal and photodynamic therapy to promote bacteria-infected wound healing using ZnO@PDA/Ag-integrated waterborne polyurethane films. *J Mater Chem B* 2025; **13**: 6177–6198.

123 Flemming HC, Wingender J, Szewzyk U, *et al.* Biofilms: An emergent form of bacterial life. *Nat Rev Microbiol* 2016; **14**: 563–575.

124 Pavlovsky L, Sturtevant RA, Younger JG, *et al.* Effects of temperature on the morphological, polymeric, and mechanical properties of *Staphylococcus epidermidis* bacterial biofilms. *Langmuir* 2015; **31**: 2036–2042.

125 Chen C, Gao Y, Qiao X, *et al.* Functional amyloid phenol-soluble modulin α1-targeting photothermal nanoplatform for effective elimination of biofilm-associated infections. *ACS Nano* 2025; **19**: 20613–20632.

126 Wang J, Yu Y, Chen L, *et al.* NIR-triggered and glucose-powered hollow mesoporous Mo-based single-atom nanozymes for cascade chemodynamic diabetic infection therapy. *Mater Today Bio* 2025; **31**: 101557.

127 Shi J, Yuan Y, Liu K, *et al.* Bilayer microneedles loading nanozymes and quantum dots with gradient photothermal antibacterial, exudate control, antioxidation, and pH monitoring for enhanced diabetic wound healing. *ACS Appl Mater Interfaces* 2025; **17**: 49317–49334.

128 Jin Y, Chu Z, Zhu P, *et al.* Double-edged dissolving microneedle patches loaded with Zn/Ce composites and vancomycin for treatment of drug-resistant bacterial infected skin abscess. *Small* 2025; **21**: 2412165.

129 Yu M, Li L, Liu Y, *et al.* Pathogenesis and treatment strategies for infectious keratitis: Exploring antibiotics, antimicrobial peptides, nanotechnology, and emerging therapies. *J Pharm Anal* 2025; **15**: 101250.

130 Barrientez B, Nicholas SE, Whelchel A, *et al.* Corneal injury: Clinical and molecular aspects. *Exp Eye Res* 2019; **186**: 107709.

131 Gurnani B, Kaur K. Recent advances in refractive surgery: An overview. *OPTH* 2024; **18**: 2467–2472.

132 Budin G, Chung HJ, Lee H, *et al.* A magnetic gram stain for bacterial detection. *Angew Chem Int Ed* 2012; **51**: 7752–7755.

133 Kong H, Li W, Tian X, *et al.* NIR-activated $FeCoO_x$ nanozymes with tri-modal synergy for multi-target uproot drug-resistant bacterial keratitis. *Chem Eng J* 2025; **521**: 166724.

134 Schwartz S, Vaziri K, Kishor K, *et al.* Endophthalmitis: State of the art. *Clin Ophthalmol* 2015; **9**: 95–108.

135 Verstappen M, Ehongo A, Cordonnier M. Postoperative endophthalmitis after cataract surgery from 2009 to 2013: A retrospective analysis at Erasme Hospital. *J Fr Ophtalmol* 2017; **40**: e103–e104.

136 Yannuzzi NA, Patel NA, Relhan N, *et al.* Clinical features, antibiotic susceptibilities, and treatment outcomes of endophthalmitis caused by*Staphylococcus epidermidis*. *Ophthalmol Retina* 2018; **2**: 396–400.

137 Sadaka A, Durand ML, Sisk R, *et al. Staphylococcus aureus* and its bearing on ophthalmic disease. *Ocular Immunol Inflamm* 2017; **25**: 111–121.

138 Ye Y, He J, Qiao Y, *et al.* Mild temperature photothermal assisted anti-bacterial and anti-inflammatory nanosystem for synergistic treatment of post-cataract surgery endophthalmitis. *Theranostics* 2020; **10**: 8541–8557.

139 Richards D. Review finds that severe periodontitis affects 11% of the world population. *Evid Based Dent* 2014; **15**: 70–71.

140 Zhang L, Wang Y, Wang C, *et al.* Light-activable on-demand release of nano-antibiotic platforms for precise synergy of thermochemotherapy on periodontitis. *ACS Appl Mater Interfaces* 2020; **12**: 3354–3362.

141 Li Y, Wang P, Liu Y, *et al.* $Fe_3O_4$-based nanospheres with high photothermal conversion efficiency for dual-effect and mild biofilm eradication against periodontitis. *ACS Appl Mater Interfaces* 2025; **17**: 14832–14845.

142 Margolis HC, Zhang YP, Lee CY, *et al.* Kinetics of enamel demineralization *in vitro*. *J Dent Res* 1999; **78**: 1326–1335.

143 Xu X, Fan M, Yu Z, *et al.* A removable photothermal antibacterial “warm paste” target for cariogenic bacteria. *Chem Eng J* 2022; **429**: 132491.

144 Kirillova A, Yeazel TR, Asheghali D, *et al.* Fabrication of biomedical scaffolds using biodegradable polymers. *Chem Rev* 2021; **121**: 11238–11304.

145 Masters EA, Ricciardi BF, Bentley KLM, *et al.* Skeletal infections: Microbial pathogenesis, immunity and clinical management. *Nat Rev Microbiol* 2022; **20**: 385–400.

146 Wu Y, Zhang X, Tan B, *et al.* Near-infrared light control of GelMA/PMMA/PDA hydrogel with mild photothermal therapy for skull regeneration. *Biomater Adv* 2022; **133**: 112641.

147 Jin J, Xu M, Liu Y, *et al.* Alginate-based composite microspheres coated by berberine simultaneously improve hemostatic and antibacterial efficacy. *Colloids Surfs B-Biointerfaces* 2020; **194**: 111168.

148 Wei H, Cui J, Lin K, *et al.* Recent advances in smart stimuli-responsive biomaterials for bone therapeutics and regeneration. *Bone Res* 2022; **10**: 17.

149 Ma K, Liao C, Huang L, *et al.* Electrospun PCL/$MoS_2$ nanofiber membranes combined with NIR-triggered photothermal therapy to accelerate bone regeneration. *Small* 2021; **17**: 2104747.

150 Zhang Y, Imamaimaiti N, Tang X, *et al.* $SiO_2$-coated ZnO for photothermal and photodynamic antibacterial applications in bone repair. *ACS Appl Bio Mater* 2025; **8**: 4766–4778.

151 Murray CJL. Findings from the global burden of disease study 2021. *Lancet* 2024; **403**: 2259–2262.

152 Fu L, Huo S, Lin P, *et al.* Precise antibiotic delivery to the lung infection microenvironment boosts the treatment of pneumonia with decreased gut dysbiosis. *Acta Biomater* 2024; **184**: 352–367.

153 Tian Z, Zhang Y, Yun J, *et al.* Advances in nanotechnology for the therapy of bacterial pneumonia. *Front Cell Infect Microbiol* 2025; **15**: 1639783.

154 Gu D, Dong N, Zheng Z, *et al.* A fatal outbreak of ST11 carbapenem-resistant hypervirulent Klebsiella pneumoniae in a Chinese hospital: A molecular epidemiological study. *Lancet Infect Dis* 2018; **18**: 37–46.

155 Liu T, Zhong G, Tang D, *et al.* Ofloxacin-loaded HMPB NPs for *Klebsiella pneumoniae* eradication in the surgical wound with the combination of PTT. *Biotech Bioeng* 2022; **119**: 1949–1964.

156 Cruz-Knight W, Blake-Gumbs L. Tuberculosis. *Primary Care-Clin Office Pract* 2013; **40**: 743–756.

157 Li B, Wang W, Zhao L, *et al.* Photothermal therapy of tuberculosis using targeting pre-activated macrophage membrane-coated nanoparticles. *Nat Nanotechnol* 2024; **19**: 834–845.

158 Ding T, Zhang L, Chen J, *et al.* "Thermal bubbles": Photothermally triggered by a carbon monoxide nanocontainer for antibiosis and immune modulation therapy. *Nano Today* 2025; **63**: 102758.

159 He X, Obeng E, Sun X, *et al.* Polydopamine, harness of the antibacterial potentials: A review. *Mater Today Bio* 2022; **15**: 100329.

160 Guo Z, Zhang Z, Zhang N, *et al.* A $Mg^{2+}$/polydopamine composite hydrogel for the acceleration of infected wound healing. *Bioactive Mater* 2022; **15**: 203–213.

161 Hu F, Zhang Y, Chen G, *et al.* Double-walled Au nanocage/$SiO_2$ nanorattles: Integrating SERS imaging, drug delivery and photothermal therapy. *Small* 2015; **11**: 985–993.

162 Hua S, Hu H, Liu J, *et al.* A mucous permeable local delivery strategy based on manganese-enhanced bacterial cuproptosis-like death for bacterial pneumonia treatment. *ACS Nano* 2024; **18**: 31923–31940.

163 Sun Z, Xiao M, Lv S, *et al.* A Ph-responsive, surface charge-switchable nanosystem with enhanced biofilm penetration for synergistic photodynamic and antibiotic therapy of diabetic wounds. *Adv Funct Mater* 2025; **35**: 2418711.

164 Liu C, Chen S, Sun C, *et al.* Protonated charge reversal nanodrugs for active targeting clearance of *Helicobacter pylori* accompanied by gut microbiota protection. *Adv Funct Mater* 2023; **33**: 2300682.

165 Ge Y, Rong F, Lu Y, *et al.* Glucose oxidase driven hydrogen sulfide-releasing nanocascade for diabetic infection treatment. *Nano Lett* 2023; **23**: 6610–6618.

166 Sun X, Wang P, Tang L, *et al.* Multifunctional hydrogel containing oxygen vacancy-rich $WO_x$ for synergistic photocatalytic $O_2$ production and photothermal therapy promoting bacteria-infected diabetic wound healing. *Adv Funct Mater* 2024; **34**: 2411117.

167 Yu L, Wu HB, Lou XWD. Self-templated formation of hollow structures for electrochemical energy applications. *Acc Chem Res* 2017; **50**: 293–301.

168 Li B, Zeng HC. Architecture and preparation of hollow catalytic devices. *Adv Mater* 2019; **31**: 1801104.

169 Yang Z, Niu Z, Lu Y, *et al.* Templated synthesis of inorganic hollow spheres with a tunable cavity size onto core–shell gel particles. *Angew Chem Int Ed* 2003; **42**: 1943–1945.